The metamorphic rocks of the Nunatak Viedma in the Southern Patagonian Andes: Provenance sources and implications for the early Mesozoic Patagonia-Antarctic Peninsula connection

Rodrigo J Suárez, Matias C Ghiglione, Mauricio Calderón, Christian Sue, Joseph Martinod, Benjamin Guillaume, Diego Rojo

Accepted Manuscript

The metamorphic rocks of the Nunatak Viedma in the Southern Patagonian Andes: Provenance sources and implications for the early Mesozoic Patagonia-Antarctic Peninsula connection

Rodrigo J. Suárez, Matías C. Ghiglione, Mauricio Calderón, Christian Sue, Joseph Martinod, Benjamin Guillaume, Diego Rojo

PII: S0895-9811(18)30337-7

DOI: https://doi.org/10.1016/j.jsames.2018.12.015

Reference: SAMES 2072

To appear in: *Journal of South American Earth Sciences*

Received Date: 10 August 2018

Revised Date: 18 October 2018

Accepted Date: 20 December 2018

Please cite this article as: Suárez, R.J., Ghiglione, Matí.C., Calderón, M., Sue, C., Martinod, J., Guillaume, B., Rojo, D., The metamorphic rocks of the Nunatak Viedma in the Southern Patagonian Andes: Provenance sources and implications for the early Mesozoic Patagonia-Antarctic Peninsula connection, *Journal of South American Earth Sciences* (2019), doi: https://doi.org/10.1016/j.jsames.2018.12.015.

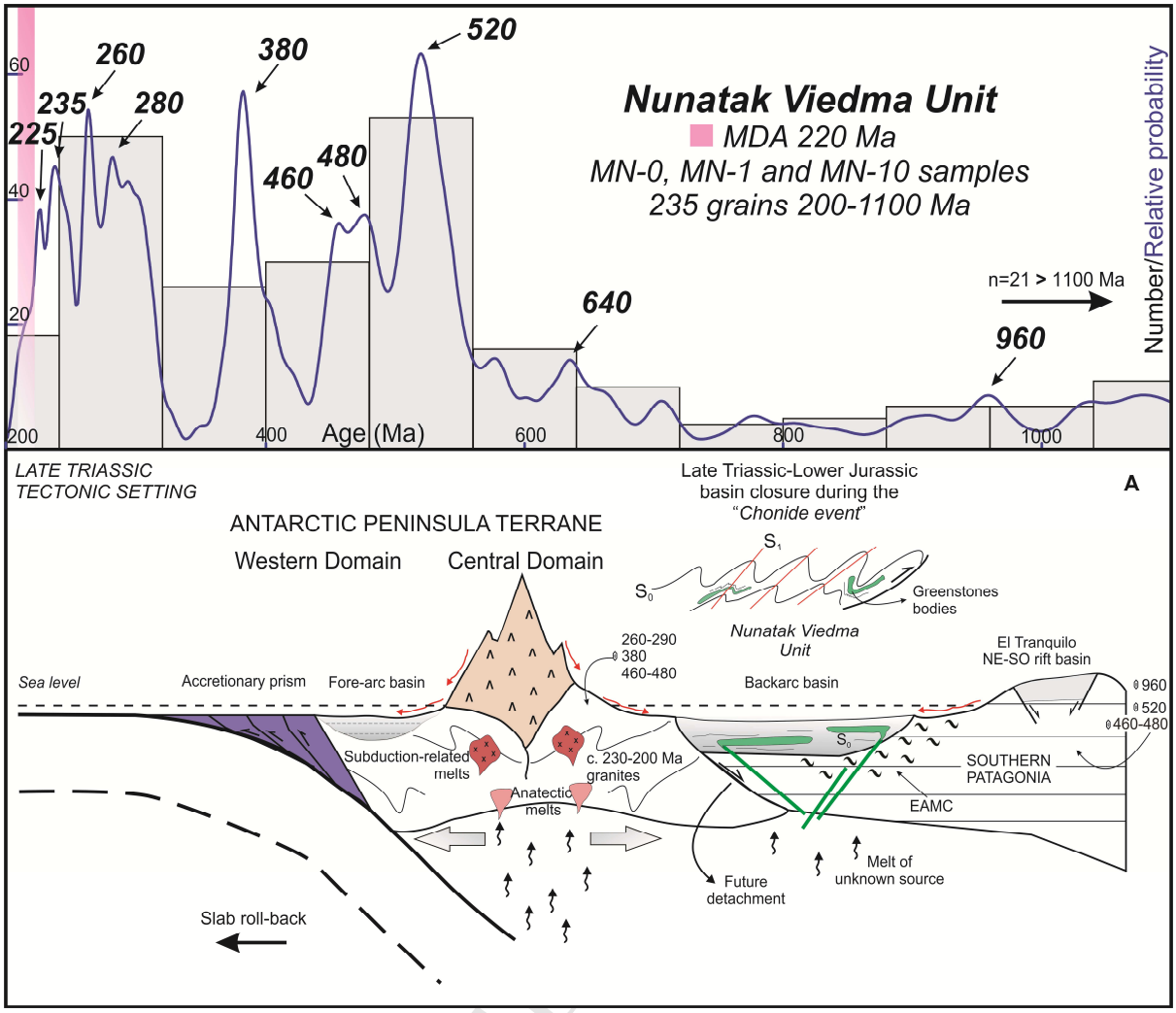

The metamorphic rocks of the Nunatak Viedma in the Southern Patagonian Andes: provenance sources and implications for the early Mesozoic Patagonia-Antarctic Peninsula connection

Rodrigo J. Suárez[a*], Matías C. Ghiglione[a], Mauricio Calderón[b], Christian Sue[c], Joseph Martinod[d], Benjamin Guillaume[e] and Diego Rojo[f]

a) Instituto de Estudios Andinos IDEAN (Universidad de Buenos Aires - CONICET), Buenos Aires, Argentina.

b) Carrera de Geología, Facultad de Ingeniería, Universidad Andrés Bello, Sazié 2119, Santiago, Chile.

c) CNRS-UMR6249, Université de Bourgogne Franche-Comté, 16 route de Gray, 25030 Besançon cedex, France.

d) ISTerre, Université de Savoie Mont-Blanc, 73376 Le Bourget du Lac cedex, France.

e) Université Rennes, CNRS, Géosciences Rennes - UMR 6118, F-35000 Rennes, France.

f) Facultad de Ingenieria y Arquitectura, Universidad Arturo Prat, Iquique, Chile.

* **Corresponding author**: Rodrigo Javier Suárez. Instituto de Estudios Andinos IDEAN (Universidad de Buenos Aires - CONICET). Intendente Güiraldes 2160 Ciudad Universitaria - Pabellón II C1428EGA – CABA Argentina. Phone: +54-298-4879805. E-mail: rodrigo_s_37@hotmail.com; rsuarez@gl.fcen.uba.ar

Abstract. The Nunatak Viedma within the Southern Patagonian Icefield has been considered as a volcanic center based on its geomorphologic features, despite the fact that field explorations by Eric Shipton determined its metamorphic nature 70 years ago. We carried out fieldwork to characterize this isolated outcrop and performed the first U-Pb dating in detrital zircons from the basement rocks located inside the Southern Patagonian Icefield. We recognized very-low grade metamorphic rocks, corresponding principally to metapelites and metapsammites, and scarce metabasites. Detrital zircons in three metapsammitic samples (composite group of 240 grains) yielded prominent age population peaks at ~1090, ~960, ~630, ~520, ~480-460, ~380, ~290-260, ~235-225 Ma that are typical of Gondwanide affinity, and youngest grains at ~208 Ma. Maximum depositional ages of 225, 223 and 212 Ma were calculated for each sample from the youngest cluster of ages. This distinctive and novelty Late Triassic age justifies differentiate the Nunatak Viedma Unit from the Devonian-early Carboniferous and Permian-Early Triassic (?) belts of the Eastern Andean Metamorphic Complex. Possible primary source areas for the detrital zircons are outcropping in southern Patagonia, the Antarctic Peninsula, and the Malvinas Islands. Additionally, secondary sources could be part of the erosion and recycling of metasediments from the Eastern Andean Metamorphic Complex. We propose that the cluster of Triassic ages is related to the volcanic arc emplaced along the Antarctic Peninsula and active at that timewhen was still attached to southern Patagonia during the Triassic. The dynamics of the early Mesozoic orogen is also discussed.

***Keywords*:** Nunatak Viedma, very-low grade metamorphic rocks, detrital zircons ages, Antarctic Peninsula, Southern Patagonian Andes, Southwestern Gondwana.

1. INTRODUCTION

55 The Nunatak Viedma located in the Southern Patagonian Icefield (Fig. 1; 49°22´S,
56 73°19´W), has been considered as an active volcano because of its geomorphologic
57 features, which resemble a group of volcanoes (Lliboutry, 1956; Mazzoni et al., 2010). The
58 early descriptions were based on the first aerial survey that covered the Patagonian icefields
59 (Lliboutry, 1956). Shipton (1960, 1963), however, undertook a field investigation between
60 1958-1962 recognizing that the Nunatak Viedma is entirely composed of metamorphic
61 rocks partially cover by quaternary deposits, mentioning that *"there was no sign whatever*
62 *of any volcanic activity"*. Nevertheless, some technical works were recently carried out to
63 characterize the composition and geomorphology of this supposed volcano (Kilian, 1990;
64 Kobashayi et al., 2010). On the other hand, mapping by the Argentine Mining Geological
65 Survey (SEGEMAR; Giacosa et al., 2012a) assigned this out crop to the late Paleozoic
66 Bahía de la Lancha Formation. By last, Blampied et al. (2012) described it as a folded
67 metasedimentary sequence composed of schists and gneisses, assigning their particular
68 geomorphological volcanic-like shape to glacial processes.

69 Metamorphic rocks of the Southern Patagonian Andes principally include low-grade,
70 metasedimentary units grouped in two distinctive, north-south oriented, Eastern and
71 Western complexes flanking the Patagonian Batholith (Hervé et al., 2003; Hervé et al.,
72 2008; Calderón et al., 2016). Deposition of the protoliths and subsequent metamorphism
73 and deformation occurred between the late Paleozoic and the early Mesozoic (Hervé et al.,
74 2008). In the widespread distributed Eastern Andean Metamorphic Complex (EAMC), the
75 protoliths were deposited during the Late Devonian-early Carboniferous and Late Permian-
76 Early Triassic (Hervé et al., 2003; Augustsson et al., 2006) and metamorphosed, at least the
77 older units, during the Gondwanide orogeny (Thomson and Hervé, 2002; Giacosa et al.,

2012; Heredía et al., 2016). In this vast metamorphic complex were included the Bahía de la Lancha and Río Lácteo formations defined in the Argentinean territory (Hervé et al., 2008). A regionally widespread angular unconformity with the overlying Upper Jurassic volcano-sedimentary rocks along the Patagonian hinterland (Giacosa and Herdia, 2004; Ghiglione et al., 2009; Giacosa et al., 2012; Zerfass et al., 2017), gives a minimum age for deformation of the folded basement units.

On the other hand, units of the western Metamorphic Complexes exhibit a geological history related to subduction dynamics and accretion of exotic terranes during the Triassic-Jurassic (Hervé et al., 2003; Hervé et al., 2008; Hervé and Fanning, 2001; Willner et al., 2009; Angiboust et al., 2017).

From correlation of Paleozoic-early Mesozoic magmatic and tecto-metamorphic events (Pankhurst et al., 2003; Hervé et al., 2006; Castillo et al., 2016; Heredía et al., 2016; Riley et al., 2016; González et al., 2018), it has been proposed that South America, Patagonia, and the Antarctic Peninsula were contiguous regions forming the SW margin of Gondwana. In this sense, several authors have discussed the spatial relation between Patagonia and the Antarctic Peninsula (Fig. 2; Suárez, 1976; Harrison et al., 1979; Lawver et al., 1998; Hervé and Fanning, 2003; Hervé et al., 2006; Ghidella et al., 2007; Calderón et al., 2016; Heredía et al., 2016) conforming the Terra Australis Orogen before Gondwana breakup (Fig. 2; Suárez, 1976; Harrison et al., 1979; Miller et al., 1987, 2007; Lawver et al., 1992, 1998; Jokat et al., 2003; König and Jokat, 2006; Ghidella et al., 2007). The "tight-fit" model of Lawver et al. (1998) suggests that the northern edge of the Antarctic Peninsula was located near the current Golfo de Penas (Fig. 2), although clear correlations between Patagonian and the Antarctic Peninsula are still missing to validate this hypothesis

(Hervé et al., 2006). After the onset of oceanic spreading, lateral displacements and block rotations during Mesozoic-Cenozoic times, including opening of the Scotia plate, determined the current plate configuration and the distribution of the continental fragments of Gondwana (Suárez, 1976; Harrison et al., 1979; Jokat et al., 2003; Eagles, 2016; Ghiglione et al., 2016).

In this contribution, we provide a lithological characterization and U-Pb zircon detrital ages from metasedimentary rocks of the Nunatak Viedma and discuss its evolution within the geodynamic context of the SW edge of Gondwana. The distinctive Late Triassic age justifies to differentiate a Nunatak Viedma Unit (NVU) separate from the EAMC. Furthermore, we discuss the possible sedimentary sources for the protolith of the NVU and its implications for the paleogeography and location of the Antarctic Peninsula with respect to Patagonia during Triassic times.

2. GEODYNAMIC CONTEXT

The Terra Australis Orogen developed along the active margin of Gondwana during Neoproterozoic-early Mesozoic times (Fig. 2; Cawood, 2005; Cawood and Buchan, 2007). At the end of the Paleozoic, several events of terrane accretion are recorded in South America (Pankhurst et al., 2006; Ramos, 2008; Calderón et al., 2016), between these the accretion of the Antarctic Peninsula terrane against Patagonia (Ramos, 2008; Calderón et al. 2016; Heredia et al. 2016), which indicate the final stages of Pangea assembly (320-250 Ma; Cawood and Buchan, 2007). Early Mesozoic tecto-magmatic events associated with continental breakup, are recorded along its SW margin (Bruhn et al., 1978; Pankhurst et al.,

2000; Riley et al., 2001; Calderón et al., 2016; González et al., 2016), related to extensional movements that started to separate the Antarctic Peninsula from southern Patagonia.

Early Mesozoic paleogeographic reconstructions suggest that the Antarctic Peninsula was located in a very close position, or even attached, to SW Patagonia (Harrison et al., 1979; Miller et al., 1987; Lawver et al., 1992, 1998; Jokat et al., 2003; Hervé et al., 2006; König and Jokat, 2006; Ghidella et al., 2007; Heredia et al., 2016). However, these models still differ in the exact paleo-latitudinal position of the Antarctic Peninsula along the Pacific margin during the Triassic or older times. Some hypothesis suggests that the northern margin of Antarctic Peninsula was located nearby Golfo de Penas (Fig. 2; Lawver et al., 1998; Hervé and Fanning, 2003; König and Jokat, 2006) or farther north, close to the 39°S, according to Heredia et al. (2016), while other reconstructions propose that the peninsula was situated either east of Patagonia or in continuity towards the south (Suárez, 1976; Miller, 2007).

Plate reconstructions from aeromagnetic data establish a southward drifting of the Antarctic Peninsula during the Jurassic (Jokat et al., 2003; König and Jokat, 2006), synchronous with rifting and oceanic floor spreading in the Rocas Verdes basin in the backarc region of Patagonia (Dalziel, 1981; Calderón et al., 2007a).

2.1. Late Paleozoic-early Mesozoic metamorphic units from southernmost South America and Antarctic Peninsula.

These units include several lower Paleozoic-Mesozoic blocks that formed the SW edge of Gondwana including possibly exotic terranes (Thomson and Hervé, 2002; Millar et al., 2002; Hervé et al., 2003, 2007, 2008; Calderón et al., 2016).

144 **2.1.1. *Southern Patagonian Andes***

145 Metamorphic rocks cropping out in the Southern Patagonian Andes (Fig. 3) can be
146 divided into (1) the **EAMC (Eastern Andes Metamorphic Complex)** along the eastern
147 flank of the Patagonian Batholith, (2) the **coastal accretionary complexes in the Pacific**
148 **archipelago**, and to a lesser extent (3) the **ophiolitic complexes of the Rocas Verdes**
149 **basin.**

150 **(1)** The **EAMC** crops out along the inner core of the South Patagonian Andes
151 (Hervé et al., 2008), including several units that compose the thick-skinned basement
152 domain towards the east (Ghiglione et al., 2009). The Bahía de la Lancha and Río Lácteo
153 formations, defined in Argentinean territory (see Giacosa and Márquez, 2002) were
154 included by Hervé et al. (2008) in this vast metamorphic unit. The EAMC mainly consists
155 in turbiditic sequences with occasional limestone bodies and metabasalt and their
156 metamorphic equivalents in greenschist facies (Hervé et al., 2008). Sedimentary protoliths
157 were deposited either in a passive margin environment (Augustsson and Bahlburg, 2003a,
158 2003b, 2008; Lacassie, 2003) or in a forearc setting (Permuy Vidal et al., 2014; Calderón et
159 al., 2016) during the Late Devonian-early Carboniferous (Augustsson et al., 2006) and
160 metamorphosed previous to the Permian (Thomson and Hervé, 2002). Giacosa et al.
161 (2012b), propose that the Bahía de la Lancha Formation was deformed during the late
162 Paleozoic Gondwanide orogeny. Additionally, the western belt of the EAMC exhibits Late
163 Permian-Early Triassic ages (Hervé et al., 2003; Augustsson et al., 2006), however its
164 deformation and metamorphism age is still unknown. High-grade metamorphic rocks and
165 migmatites located on the western border of the EAMC resulted fron the emplacement of

Late Jurassic granitoids of the South Patagonian Batholith (Hervé et al., 2007; Calderón et al., 2007b).

(2) The **Coastal accretionary-subduction complexes** (Fig. 3) include (see Hervé *et al*., 2008, Calderón et al., 2016) the CMC (Chonos Metamorphic Complex), the MDAC (Madre de Dios Accretionary Complex) and the DAMC (Diego de Almagro Metamorphic Complex).

The CMC from the Chonos Archipelago is composed of metaturbidites and metabasites and meta-cherts in minor quantities (Hervé et al., 2008). The protolith was deposited during the Late Triassic (Fang et al., 1998; Hervé and Fanning, 2001) and subsequently affected by metamorphism and deformation during Late Triassic-Early Jurassic times, possibly related to the Chonide deformational event (Hervé et al., 2006, 2008). The high-pressure/low-temperature metamorphism is typical of accretionary prisms (Willner et al., 2000; Ramírez-Sánchez et al., 2005).

The MDAC includes three lithostratigraphic units known as: (i) the Tarlton limestone, composed by a massive pelagic limestone body deposited during the late Carboniferous-early Permian, (ii) the Denaro Complex represented by pillow basalts and radiolarian cherts, and (iii) the Duque de York Complex composed by turbiditic successions unconformably deposited over the Tarlton limestone and Denaro Complex (Forsythe and Mpodozis, 1979, 1983). The lower-middle Permian Duque de York Complex (Faundéz et al., 2002) experienced low-grade metamorphic conditions during the Early Jurassic, possibly related to an accretionary event (Thomson and Hervé, 2002). The Denaro

and Tarlton complexes have generally been interpreted as oceanic exotic terranes (Faundéz et al., 2002; Rapalini et al., 2001).

The DAMC corresponds to the assemblage of two metamorphic units tectonically juxtaposed by the Puerto shear zone: the Almagro HP-LT Complex composed by metamafic volcanic rocks with scarce metasedimentary rocks and the Lazaro Unit with seafloor-derived metamafic and metasedimentary rocks (Angiboust et al., 2017). The protolith of these high-pressure rocks have been deposited in the Late Jurassic and metamorphosed as part of an accretionary wedge that was active during the Cretaceous (Hervé and Fanning, 2003; Hyppolito et al., 2016; Angiboust et al., 2017, 2018).

(3) Ophiolitic complexes of the Rocas Verdes basin consist of sequences of massive and layered gabbros, sheeted dykes and basalts with oceanic affinity, whereas ultramafic rocks are absent (Stern and De Witt, 2003; Calderón et al., 2007a). From north to south they are the Sarmiento Complex in the Southern Patagonian Andes and the Capitán Aracena and Tortuga complexes in the Fuegian range (Stern and De Witt, 2003; Calderón et al., 2013). These rocks were emplaced during the Late Jurassic-Early Cretaceous in a backarc rift basin (Calderón et al., 2007). The subsequent basin closure and obduction occurred during the Cenomanian-Coniacian (Calderón et al., 2007a; Klepeis et al., 2010; Calderón et al., 2012), producing a major advance of the orogenic front and a wedge-top setting for the adjacent Austral-Magallanes basin depocenter (Fosdick et al., 2011; Likerman et al., 2013; Ghiglione et al., 2014, 2016).

2.1.2. *Tierra del Fuego*

Metamorphic rocks of the Cordillera Darwin and extra-Andean region are known as **Cordillera Darwin Metamorphic Complex** and **Tierra del Fuego Igneous and Metamorphic Complex** (Fig. 3), respectively. At Cordillera Darwin the clastic protolith of the metasedimentary units were deposited in the Paleozoic (Hervé et al., 1981a, 2010b; Barbeau et al., 2009b) and their detrital zircon age spectra are comparable with those of the EAMC (Barbeau et al., 2009b; Hervé et al., 2010b). These metamorphic rocks are unconformably overlain by Jurassic volcaniclastic rocks, and the whole succession has been strongly deformed and metamorphosed in the Cretaceous by the Andean Orogeny (Hervé et al., 2010b; Maloney et al., 2011). The extra-Andean region of Tierra del Fuego is characterized by Cretaceous–Cenozoic sedimentary rocks of the Austral-Magallanes basin (e.g. Ghiglione et al., 2010). Underlying foliated plutonic rocks (orthogneisses) and migmatitic gneisses were detected in boreholes. These rocks have Cambrian crystallization ages and are affected by a late Permian magmatic-anatectic event (Sölner et al., 2000; Calderón et al., 2010; Hervé et al., 2010a; Castillo et al., 2017).

2.1.3. *Antarctic Peninsula*

Basement rocks from the Antarctic Peninsula at Graham Land and Palmer Land yield *in situ* ages ranging from Ordovician to Late Triassic (Fig. 3; Millar et al., 2002; Riley et al., 2012).

In this region, three geological domains separated by shear zones are recognized (Fig. 3; Vaughan and Storey, 2000; Ferraccioli et al., 2006; Burton-Johnson and Riley, 2015). The Permian-Upper Triassic to Lower Jurassic Central domain is composed by subduction-related granites, orthogneiss and migmatites cropping out in Palmer Land area

(Wever et al., 1994; Millar et al., 2002; Riley et al., 2012). The Eastern domain includes the Permian to Triassic **TPG (Trinity Peninsula Group)**, whose age is constrained by U-Pb dating in detrital zircons and stratigraphic relationships (Carvalho et al., 2005; Barbeau et al., 2009a; Castillo et al., 2016). This group has been divided into the Hope Bay, View Point and Legoupil formations composed of metaturbidites and metapillow lavas deposited in a forearc basin (Hyden and Tanner, 1981). Unconformably overlain on the TPG, Heredía et al. (2016) redefine the uppermost Düse Bay Formation described by Del Valle et al. (2007) as a synorogenic succession deposited in a retroarc foreland basin and related to the Tabarin Permian-Triassic orogeny. To the northeast of the Antarctic Peninsula, the South Orkney Island (Fig. 3) at the southern limb of the Scotia Range exhibits outcrops of the **Greywacke-shale Formation** interpreted as a possible Triassic equivalent of the TPG (Dalziel, 1982; Trouw et al., 1997).

3. METAMORPHIC ROCKS OF THE NUNATAK VIEDMA UNIT

3.1. *Field and petrographic lithological characterization*

The rocky out crop of the Nunatak Viedma is modeled by glaciary processes and presents no evidence of volcanic activity. The rocks correspond mainly to metapsammites, metapelites and scattered interleaved metabasites (Fig. 6). The metapsammites are gray, present scarce clasts of both felsic volcanic rocks and granites and pumice wisps with tube vesicle texture. In all samples, grains of quartz, white mica, and plagioclase are dominant (Fig. 7A) with scarce K-feldspar and accessories like zircon, tourmaline, apatite, and titanite. The minerals are distributed in the quartz-plagioclase and quartz-white mica domains, which are interpreted as remnants of a prior sedimentary lamination (S_0).

Sometimes the mechanically reoriented and kinked detrital mica together with dissolution films define a diagenetic foliation (*sensu* Passchier and Trouw, 2005). The metamorphic mineral assemblage is composed of quartz, chlorite, white mica and carbonate (Fig. 7B). The fine bands formed by intergrowths of white mica and chlorite define the S_1 foliation (Fig. 7B, 7C). Chlorite locally replaces white mica and also is present as porphyroblasts. The mica-rich domains, consisting of white mica and chlorite, are affected by a poorly developed crenulation cleavage (S_2; Fig. 7C). By last, the rocks are crosscut by veinlets of carbonate and quartz.

The metabasites preserve amygdaloidal and porphyritic primary textures (Fig. 7D). Primary igneous phases are composed of plagioclase, clinopyroxene, pseudomorphs of olivine and opaques (Fig. 7D). Metamorphic mineral assemblages vary between samples; the most common are: i) chlorite, smectite, zeolite and carbonates (Fig. 7D); ii) chlorite, pumpellyite (?); iii) actinolite, chlorite; and iv) smectite, quartz, and carbonate. These minerals occur in amygdules and micro-veinlets, or as the alteration product of plagioclase.

3.2. *Estimations of metamorphic P-T conditions*

Deformation processes associated to micro-structures, identification of metamorphic mineral assemblages and their comparison with petrogenetic grids for metabasites (Schiffman and Day, 1999) and with typical metamorphic mineral assemblage for metapelites (Bucher and Grapes, 2011), indicate that metamorphism during deformation and developments of S_2 foliation progressed in very low to low-grade conditions.

The textural equilibriums among white mica + chlorite + quartz + carbonate in metapsammites indicate a sub-greenschist facies of metamorphism (chlorite zone), with estimated temperatures at 200-300° C and pressures between 1.5 and 3.0 kbar.

The mineral assemblage identified in the metabasites indicate a formation temperature of 180-230° C and variable pressures between 1 and 3 kbar to chlorite + pumpellyite mineral association, while the appearance of actinolite could be point out temperatures greater than 300° C. These physical conditions correspond to the transition between sub-greenschist and greenschist facies.

4. U-PB ZIRCON DETRITAL AGES IN METASEDIMENTARY ROCKS

4.1. Analytical techniques

Three samples were taken in site 49°25'50"S/ 73°18'30"W (Fig. 1) to analyze detrital zircons by U-Pb method in the Washington State University Laboratory, following the methodology described in Chang et al. (2006). Approximately three hundred zircon grains were separated from a total of 5 kg of three metapsammites (samples MNO, MN1 and MN10). Heavy mineral fractions were concentrated and separated into 100, 150 and 250 mm size fractions by standard crushing and panning. Zircon fractions of roughly 400 grains were handpicked in alcohol under a binocular microscope for geochronology analysis. Zircons of unknown ages and standards were handpicked under the microscope and mounted in a 1-inch diameter epoxy puck and slightly ground and polished to expose the surface and keep as much material as possible for laser ablation analyses. After cathodoluminescence imaging, the LA-ICP-MS U-Pb analyses were conducted using a New Wave Nd: YAG UV 213-nm laser coupled to a Thermo Finnigan Element 2 single

294 collector, double-focusing, magnetic sector ICP-MS. Laser spot size and repetition rate
295 were 30 microns and 10 Hz, respectively. He and Ar carrier gases delivered the sample
296 aerosol to the plasma. Each analysis consists of a short blank analysis followed by 250
297 sweeps through masses 202, 204, 206, 207, 208, 232, 235, and 238, taking approximately
298 30 s. Time-independent fractionation was corrected by normalizing U/Pb and Pb/Pb ratios
299 of the unknowns to the zircon standards (Chang et al., 2006). U and Th concentration were
300 monitored by comparing to NIST 610 trace element glass. Two zircon standards were used:
301 Plesovice, with an age of 338 Ma (Sláma et al., 2008) and FC-1, with an age of 1099 Ma
302 (Paces and Miller, 1993). Uranium-lead ages and plots were calculated using Isoplot
303 (Ludwig, 2003). Analyses were corrected assuming concordance and applying a common
304 Pb correction using the 207 Pb method (Williams, 1998).

305 The analytical data with concordant ages are reported in the **Supplementary Data**,
306 including uncertainties at the 1σ level, and measurement errors. Best ages were chosen
307 based on the precision of the isotopic systems, thus $^{206}Pb/^{238}U$ ages were selected for
308 zircons younger than 1200 Ma and $^{207}Pb/^{206}Pb$ ages for older ones (Gehrels et al., 2008). In
309 a first step, all ages were plotted in the Tera and Wasserburg (1972) Concordia diagram
310 (Fig. 4). Afterward, a filtering was applied to assess discordant ages, which can be
311 quantified using the ratio between $^{206}Pb/^{238}U$ and $^{207}Pb/^{206}Pb$ ages (Fig. 4; Wetherill, 1956;
312 Spencer et al., 2016). The resulting percentage of "discordance" was set at 20% as
313 commonly used for detrital zircons (e.g. Nelson and Gehrels, 2007; Naipauer et al., 2010;
314 among many others).

315 **4.2. Estimation of maximum depositional age**

316 Obtaining the MDA (maximum depositional age) of a geological unit is one of the
317 most widely used applications of detrital zircon geochronology and can be calculated from
318 different methods (Dickinson and Gehrels, 2009). The age of the youngest zircon from a
319 data set gives some insights, but uncertainty on the precision of a single age is still large
320 since it does not allow a statistical or modal test (Dickinson and Gehrels, 2009; Gehrels,
321 2014). Other methodologies provide more conservative estimations and have turned out
322 coherent in units with biostratigraphic control, as the weighted mean age of a cluster
323 composed by the three (or more) youngest zircons whose σ errors overlap (Dickinson and
324 Gehrels, 2009). We applied this methodology to calculate a conservative MDA from each
325 sample, and the average of these three ages was assumed as the MDA of the unit.

326 **4.3. Detrital zircon features and U-Pb data**

327 In all the analyzed samples the pattern of detrital ages, external morphology of the
328 detrital zircon grains and Th/U ratio are very similar. For this reason, they will be described
329 as a unique set. Figure 5 shows the distribution of detrital zircon ages for each sample and
330 the probability plots and associated maximum depositional age estimations.

331 About one hundred zircon grains were analyzed from each sample but only 79 of 101
332 (MN0), 94 of 112 (MN1) and 83 of 100 (MN10) zircons grains with discordance values
333 <20% endured filtering. Concordant zircon ages define a complex pattern of detrital ages
334 that range from the Archean to the Late Triassic (Fig. 5).

335 Detrital zircon grains are 50-260 µm in length (median length is 114 µm) and their
336 external morphology exhibits different classes (according to Gärtner et al., 2013),
337 concentrated in stubby- and stalky-types. The Th/U ratios show values between 0.05-2.47;

in all samples the Th/U is at least 87% greater than 0.2, indicating an igneous origin for most of them.

The age distribution of detrital zircon grains include representative Paleozoic-early Mesozoic (65%), Proterozoic (34%) and isolated Archean ages (1%; Fig. 5). The peaks of detrital ages define five main groups in the Paleozoic-Mesozoic: Early Cambrian (~520 Ma), Early-Middle Ordovician (~480-460 Ma), Late Devonian (~380 Ma), Permian (~290-260 Ma) and Triassic (~235-225 Ma). Precambrian ages are concentrated in the Neoproterozoic around ~1090 Ma, ~960 Ma, and ~630 Ma. MDAs are Late Triassic, at 225 Ma for MN-0, 212 Ma for MN-1 and 223 Ma for MN-10 (Fig. 5), with errors within ± 5 Ma.

5. DISCUSSION

In a first approach, the metamorphic rocks of the Nunatak Viedma could be included as part of the EAMC on the basis of its geographical proximity and lithological similarities. However, the Late Triassic peak of U-Pb zircon detrital ages clearly differentiates a new tectonostratigraphic unit in the *collage* of pre-Andean metamorphic belts of the Southern Patagonian Andes. We propose to denominate these rocks as Nunatak Viedma Unit (NVU). Based on petrographic and geochronological data, the geological significance of the NVU and its possible correlations with other metamorphic complexes of the southwestern edge of Gondwana in the early Mesozoic, are discussed below.

5.1. Provenance sources and paleogeographic implications

In quartz-rich metapsammites, with a fine-grained terrigenous, probably turbiditic protolith, detrital zircon populations of Late Triassic, Paleozoic (Cambrian, Ordovician, Devonian, Permian), Neoproterozoic and isolated Archean ages were identified.

Archean and Proterozoic detrital zircon ages have been previously identified in metamorphic complexes located along the Patagonian Andes, for example in the EAMC (Hervé et al., 2003; Augustsson et al., 2006). However, Patagonia as a primary (igneous) cratonic source of detrital zircons still remains under discussion, because of the lack of magmatic outcrops of that age. Precambrian primary source areas are located in South America north of Patagonia, Africa and East Antarctica (cf. Hervé et al., 2003; Augustsson et al., 2006), and we consider these primary sources areas to be located too far north and east to have reach the NVU basin directly. For this reason, Precambrian detrital ages identified within the Triassic NVU, can be more easily explained by recycling of the nearby EAMC and also from other Paleozoic igneous-metamorphic complexes with outcrops in surrounding areas, probably exposed at the time of NVU deposition.

Recent works consider the Malvinas Islands and southern Patagonia as a single continental block (Ramos et al., 2017; Schilling et al., 2017). From that perspective, Mesoproterozoic Grenvillian sources could correspond to granites and gneisses of the Cabo Belgrano Complex, which are cropping out in the Malvinas islands (Fig. 3b; Cingolani and Varela, 1976; Rex and Tanner, 1982; Thomas et al., 2000) and possibly in the neighboring Argentinean Atlantic platform (Wareham et al., 1998; Chemale Jr. et al., 2018).

On the other hand, Paleozoic and Mesozoic detrital zircons could potentially come from multiple sources (Fig. 3a, b). The early Cambrian zircon ages, related to the Pampean

orogen in center and northwest Argentina and the Ross-Delamerian orogen in northern Patagonia (Ramos and Naipauer, 2014; González et al., 2018) and Antarctic-Australia (Cawood and Buchan, 2007). In the North Patagonian Massif, the low-grade (Nahuel Niyeu and El Jagüelito formations) and high-grade (Mina Gonzalito Complex) metamorphic units and the Tardugno Granodiorite present Cambrian ages (Fig. 3b; Pankhurst et al., 2006; González et al., 2011; Rapalini et al., 2013; Greco et al., 2017). Cambrian gneisses and foliated plutonites, pertaining to the Tierra del Fuego Igneous and Metamorphic Complex, have been identified in exploratory boreholes of the Austral-Magallanes basin (Söllner et al., 2000; Hervé et al., 2010a). The crystallization age of these igneous rocks was calculated at around of 520 Ma (Söllner et al., 2000; Pankhurst et al., 2003; Hervé et al., 2010a), it turns out to be highly coincident with early Cambrian peak presents in our samples.

Detrital ages grouped at ~460-480 Ma peaks could be sourced from Lower to Middle Ordovician granitoids of the Punta Sierra Plutonic Complex in the North Patagonian Massif (Fig. 3b; Pankhurst et al., 2006; González et al., 2008, 2014) and the Río Deseado Complex in the Deseado Massif (Loske et al., 1999; Pankhurst et al., 2003). Also, basement outcrops in Graham Land at the Antarctic Peninsula are composed of dioritic gneisses with Ordovician ages (Fig. 3a; Riley et al., 2012).

The Devonian peak could be associated with widely represented igneous rocks in the Northern Patagonian Andes (Varela et al., 2005; Pankhurst et al., 2006; Hervé et al., 2016) and in the western part of the North Patagonian Massif (Hervé et al., 2016). These ages are poorly represented in the Southern Andes, Antarctic Peninsula (Millar et al., 2002; Pankhurst et al., 2003) and in the Deseado Massif (Pankhurst et al., 2003). Devonian

detrital ages are also common in the EAMC (Augustsson et al., 2006) and in metamorphic rocks from the western Deseado Massif (Permuy Vidal et al., 2014).

An important Permian-Triassic zircon population suggests erosion of post-Gondwanan igneous rocks and of a late Paleozoic-early Mesozoic magmatic arc active during sedimentation of the NVU. An alternative explanation to the Permian detrital ages could be the recycling from the western belt of the EAMC. Permian Igneous rocks (~280-250 Ma) has been identified in the North Patagonian Massif (Fig. 3b; Pankhurst et al., 2014), although plutonic samples of that age are scarce in southern Patagonia. Recently, new zircon U-Pb radiometric data obtained principally in the Antarctic Peninsula, but also some in Tierra del Fuego (Calderón et al., 2010; Hervé et al., 2010a; Millar et al., 2012; Castillo et al., 2017) demonstrates a widespread distributed Permian metamorphic-magmatic event. Castillo et al. (2016) studied Permian to Triassic metasedimentary rocks from the Pacific coast of SW Chile using isotope analyses in detrital zircon grains and they suggested the Permian subduction-related magmatic arc located in Patagonia and west Antarctic as an important source.

From a paleogeographic point of view, plutonic rocks (between 236-200 Ma by Millar et al. 2002 and Riley et al. 2012) from the Antarctic Peninsula arc, located to the W and SW (Fig. 3a) were the closest possible source for Triassic detrital zircons (235-208 Ma) during sedimentation of the protolith of the NVU, taking into account the hypothesis that the Antarctic Peninsula was attached to Patagonia at that time (Fig. 2; Calderón et al. 2016; Castillo et al., 2016; Heredía et al., 2016).

In summary, U-Pb analysis in detrital zircons from the NVU show a wide distribution of ages with all Paleozoic to early Mesozoic periods very well represented, as well as an important Proterozoic component (Figs. 5 and 8). The diverse although equitable zircons distribution (Fig. 5) can only be explained by considering a multiplicity of sources for the Proterozoic-Paleozoic components, located in Patagonia and Antarctic Peninsula (Fig. 3a, b). We propose that the very well represented and particular Permian-Triassic group of ages (Figs. 5 and 8) was sourced from the active magmatic arc emplaced onto the Trinity Peninsula Group along Antarctic Peninsula.

5.2. Nature, age, and correlations of the Viedma basin

If we consider the petrography, and particularly the detrital zircon age spectra (*sensu* Cawood et al., 2012) as an expression of the tectonic setting of the NVU protolith, i.e. the Viedma basin , their distribution indicate a basin flanked by an active Late Triassic magmatic arc (Fig. 9). In order to further define the nature of this basin and its position with respect to the recognized Triassic magmatic arcs is necessary to take into account the regional correlation with other contemporaneous metamorphic units.

Metamorphic belts with protoliths of Triassic age are rare in the Patagonian Andes, except by the CMC located in the present forearc about 300-400 km to the northwest of the NVU (Fig. 3). Detrital zircons ages (Hervé and Fanning, 2001) and fossils record (Fang et al., 1998), constraint the sedimentation age in a Late Triassic basin, within an environment of accretionary wedge (Hervé et al., 1981b; Hervé, 1988), here onwards called the “Chonos basin”.

444 The distribution pattern of detrital ages of the CMC and NVU shows that both
445 basins were mainly fed by Permo-Triassic sources, although the NVU exhibits particular
446 Neoproterozoic, Cambrian, and Ordovician detrital ages probably sourced from the
447 Patagonian massifs (see section 5.1.). Trench or forearc basins such as the Chonos basin,
448 present a large population of detrital ages close to the sedimentation age without large
449 proportions of older zircon grains, while basins in a retroarc position present an input of
450 older detrital sources from the adjacent basement outcrops (Fig. 9; Cawood et al., 2012).
451 Given the broad range of detrital ages found in the NVU, it seems that the Viedma basin
452 was probably a retroarc position (Fig. 10).

453 Conscious of the difficulty that represent to infer paleogeography from provenance
454 data due to the complexity of the drainage systems and their catchment areas (Cawood et
455 al., 2003), the Triassic volcanic arc emplaced along Antarctic Peninsula, and possibly with
456 continuation in Central Patagonia (i.e. Central Patagonian Batholith and Curaco Plutonic-
457 Volcanic Complex, with ages between 222-206 Ma; Rapela et al., 1992; Saini Eidukat et
458 al., 2004; Zaffarana et al., 2014), could have played the role of topographic barrier between
459 both compared basins. In this way, the Viedma basin caught Neoproterozoic, Cambrian and
460 Ordovician zircon grains sourced from extra-andean Patagonian basement highs sources
461 located to the east, while Chonos basin was fed by the flanking Triassic arc and the
462 underneath host rock.

463 **5.3. Early Mesozoic dynamics of the subduction system**

464 Accretionary orogens were traditionally classified according with their surrounding
465 subduction style, considering and linking mainly slab dip angle, strain class in the upper

plate and trench migration (Uyeda and Kanamori, 1979; Jarrard, 1986; Stern, 2002; Heuret et al., 2007; Ramos, 2010). In this context, two end-members have been identified: advancing and retreating orogens (*sensu* Cawood et al., 2009). In the second case, the dynamics of the orogen (see more in Collins, 2002a) induce lithospheric extension and the development of backarc basins (Collins, 2002b; Cawood et al., 2009). The early Mesozoic arc-backarc system established along of the west margin of Patagonia and Antarctic Peninsula shows close relationship with this kind of accretionary orogen undergoing extension.

Early Mesozoic orthogneisses and foliated granites emplaced along Antarctic Peninsula (mainly in the Central Domain) were interpreted as products derived from the subduction zone but during a regime of lithospheric extension (Wever et al., 1994). Likewise, the Late Triassic in Patagonia and along of the western margin from South America was characterized by extension during ongoing subduction (Franzese and Spalletti; 2001; Giambiagi et al., 2009; Giacosa et al., 2010; Spikings et al., 2016; González et al., 2017). Its simultaneity with the development of the Viedma basin supports our hypothesis of an extensional aperture of the Viedma basin during the Late Triassic (Fig. 10).

Folded basement rocks around Paso del Viento that we assign to the NVU on the basis of lithological affinity (Fig. 1) and are overlain in angular unconformity by Upper Jurassic volcanic rocks from El Quemado Complex (153-162 Ma by Pankhurst et al., 2000). Such stratigraphic relations can indirectly constraint the Viedma basin closure, deformation, and metamorphism, between the Late Triassic and the Middle Jurassic (Fig. 11). Regionally, this deformational event can be related to the Late Triassic (?)-Early

Jurassic Chonide accretionary event (Fig. 11; Thomson and Hervé, 2002; Hervé et al., 2008), which affected the CMC and the Central Patagonian region (Fig. 11; Zaffarana et al., 2014), and was synchronous with the Peninsula orogeny in the Antarctic Peninsula (Fig. 11; Vaughan and Livermore, 2005; Hervé et al., 2006). Overall our tectonic reconstruction marks a tectonic mode switching from Late Triassic extension (or transtension?) to Early Jurassic contraction (Fig. 11).

In southernmost Patagonia, towards the latest Jurassic new evidences of extension and establishment of a backarc setting are registered in the Rocas Verdes basin (Fig. 11; cf. Calderón et al., 2007a), which located southwest from NVU. This means an oceanward migration of the arc-backarc system after the deformation (closure) of the NVU. Whereas at Central Patagonia also registers, from the Late Triassic to Early Cretaceous, a westward migration of the arc magmatism, in fact, this arc magmatism develops during a period of upper plate extension (Echaurren et al., 2016). This pattern of arc-backarc system younger outboard associated to extension, disrupted by short-lived deformation events, were features identified as typical from retreating orogens (Collins, 2002a, 2002b; Cawood et al., 2009).

Even though the dynamics of the Mesozoic orogenic system could be reflecting a retreating-mode, in southernmost Patagonia, its evolution is quite complex and was influenced by the connection with the Antarctic Peninsula (Hervé and Fanning, 2003; Calderón et al., 2007a). The Jurassic arc magmatism emplaced along the Patagonia-Antarctic Peninsula (Hervé et al., 2007; Echaurren et al., 2016; Riley et al., 2016), was synchronous with the Middle-Late Jurassic extensional-transtensional movements that started to separate the Antarctic Peninsula composite terrane (magmatic arc and forearc

512 setting) from Patagonia (König and Jokat, 2006). Indeed, the lithospheric extension finally
513 resulted in the appearance of oceanic floor in the Weddell Sea at ~160-147 Ma (Fig. 11; see
514 discussion in Ghidella et al., 2007) and the partial separation between both blocks,
515 concomitant with the development of the Rocas Verdes basin. Finally, towards Cretaceous
516 times, the rocks of the southernmost Chilean margin were involved in the process of
517 subduction (Hervé and Fanning, 2003; Angiboust et al., 2018) revealing that Antarctic
518 Peninsula was located farther south from Patagonia (Hervé and Fanning, 2003).

519 **6. CONCLUSIONS**

520 We propose a new lithostratigraphic unit, in the Southern Patagonian Ice Field, and
521 also recognized in the upper parts of the surrounding cordillera (Fig. 1) characterized by
522 very-low grade metamorphic rocks of Late Triassic age. It is the first mention of Triassic
523 metamorphic rocks in Argentina.

524 We discard a volcanic origin to the Nunatak Viedma and we separate these rocks
525 from similar rocks assigned to the Bahía de la Lancha Formation by age and lithology.

526 These Upper Triassic very low- to low-grade metamorphic rocks would integrate a
527 metamorphic inlier that we propose to denominate “Nunatak Viedma Unit”. It is a key
528 element to understand the Patagonia-Antarctic Peninsula geometrical fit and the evolution
529 of the early Mesozoic orogenic system. Given its broad range of detrital ages, it seems that
530 the Viedma basin was probably a extensional retroarc-backarc basin, separated from trench-
531 forearc basins such as the Chonos basin by an active volcanic arc emplaced along Central
532 Patagonia and the Antarctic Peninsula.

533 **ACKNOWLEDGMENTS**

This work has been carried out thanks to the financial support of grants projects Agencia PICT-2013-1291; CONICET PIP 2014-2016 GI directed by M.G., Argentinian-French ECOS-SUD project A15U02 (CS and MG), and Proyecto FONDECYT No. 1161818 to MC. The authors are grateful to Parques Nacionales of Argentina for granting permission to access and study Los Glaciares National Park. RS is grateful to Dr. Pablo González (UNRN-CONICET) for comments and suggestions about the U-Pb geochronology. Likewise, we are thankful to both reviewers and the editor of the journal to spend time checking the work. This is contribution R-274 of the Instituto de Estudios Andinos Don Pablo Groeber (UBA-CONICET).

REFERENCES

Angiboust, S., Cambeses, A., Hyppolito, T., Glodny, J., Monié, P., Calderón, M., Juliani, C., 2018. A 100-m.y.-long window onto mass-flow processes in the Patagonian Mesozoic subduction zone (Diego de Almagro Island, Chile). The Geological Society of America. https:// doi .org /10 .1130 /B31891 .1

Angiboust, S., Hyppolito, T., Glodny, J., Cambeses, A., Garcia-Casco, A., Calderón, M., Juliani, C., 2017. Hot subduction in the middle Jurassic and partial melting of oceanic crust in Chilean Patagonia. Gondwana Research, 42, 104-125. https://doi.org/10.1016/j.gr.2016.10.007.

Augustsson, C., Bahlburg, H., 2003a. Active or passive continental margin? Geochemical and Nd isotope constraints of metasediments in the backstop of a pre-Andean accretionary wedge in southernmost Chile (46°30' – 48°30'S). In: Mc.Cann, T., Saintot, A. (Eds.), Tracing Tectonic Deformation Using the sedimentary record. Geological Society of London, Special Publications, 253-268. DOI: 10.1144/GSL.SP.2003.208.01.12.

Augustsson, C., Bahlburg, H., 2003b. Cathodoluminescence spectra of detrital quartz as provenance indicators for Paleozoic metasediments in southern Andean Patagonia. Journal of South American Earth Sciences, 16, 15-26. https://doi.org/10.1016/S0895-9811(03)00016-6.

Augustsson, C., Bahlburg, H., 2008. Provenance of late Palaeozoic metasediments of the Patagonian proto-Pacific margin (southernmost Chile and Argentina). International Journal of Earth Sciences, 97, 71-88. DOI: 10.1007/s00531-006-0158-7

Augustsson, C., Münker, C., Bahlburg, H., Fanning, M. 2006. Provenance of late Palaeozoic metasediments of the SW South American Gondwana margin: a combined U–Pb and Hf-isotope

565 study of single detrital zircons. Journal of the Geological Society, 163, 983-995.
566 https://doi.org/10.1144/0016-76492005-149.

567 Barbeau, D.L., Davis, J.T., Murray, K.E., Valencia, V., Gehrels, G.E., Zahid, K.M., Gombosi, J.,
568 2009a. Detrital-zircon geochronology of the metasedimentary rocks of northwestern Graham
569 Land. Antarctic Science, 22, 1, 65–78.

570 Barbeau, D.L., Olivero, Swanson-Hysell, N.L., Zahid, K.M., E. B., Murray, K.E., Gehrels, G.E.
571 2009b. Detrital-zircon geochronology of the eastern Magallanes foreland basin: Implications for
572 Eocene kinematics of the northern Scotia Arc and Drake Passage. Earth and Planetary Science
573 Letters, 284, 3-4, 489-503.

574 Blampied, J., Barberón, V., Ghiglione, M., Leal, P., Ramos, V., 2012. Disambiguation of the
575 nunatak Viedma: a basement block previously confused as a volcanic center. In: XXIII Congreso
576 Geológico Chileno. Antofagasta, Chile, 380-382.

577 Bruhn, R.L., Stern, C.R. and De Wit, J.J., 1978. Field and geochemical data bearing on the
578 development of a Mesozoic volcanic-tectonic rift zone and back-arc basin in southernmost South
579 America. Earth and Planetary Science Letters, 41, 32-46.

580 Bucher, B., Grapes, R., 2011. Petrogenesis of Metamorphic Rocks, eighth ed. Springer-Verlag,
581 Berlín, 428 pp.

582 Burton-Johnson, A., Riley, T.R., 2015. Autochthonous v. accreted terrane development of
583 continental margins: a revised in situ tectonic history of the Antarctic Peninsula. Journal of the
584 Geological Society, 172, 4, 822-825. https://doi.org/10.1144/jgs2014-110.

585 Calderón, M., Fildani, A., Hervé, F., Fanning, M.C., Weislogel, A., Cordani, U., 2007a. Late
586 Jurassic bimodal magmatism in the northern sea-floor remnant of the Rocas Verdes basin,
587 southern Patagonian Andes. Journal of the Geological Society, 164, 1011–1022.

588 Calderón, M., Fosdick, J.C., Warren, C., Massone, H-J., Fanning, C.M., Fadel Cury, L.,
589 Schwanethal, J., Fonseca, P.E., Galaz, G., Gaytán, D., Hervé, F., 2012. The low-grade Canal de
590 las Montañas Shear Zone and its role in the tectonic emplacement of the Sarmiento Ophiolitic
591 Complex and Late Cretaceous Patagonian Andes orogeny, Chile. Tectonophysics, 524-525, 165-
592 185. https://doi.org/10.1016/j.tecto.2011.12.034.

593 Calderón, M., Hervé, F., Fuentes, F., Fosdick, J. C., Sepúlveda, F., Galaz, G., 2016. Tectonic
594 Evolution of Paleozoic and Mesozoic Andean Metamorphic Complexes and the Rocas Verdes
595 Ophiolites in Southern Patagonia. In: Ghiglione, M.C. (Ed.), Geodynamic Evolution of the
596 Southernmost Andes. Springer Earth System Sciences, 7-36. https://doi.org/10.1007/978-3-319-
597 39727-6_2.

598 Calderón, M., Hervé, F., Massonne, H-C., Fanning, C.M., Chavez, A., Pankhurst, R., Kraus, S.,
599 2010. Zircon crystallization in low-pressure anatectic systems: Constraints from Permian
600 migmatites of Tierra del Fuego, southernmost South America. In XII South American
601 Symposium on Isotope Geology. Brasília.

Calderón, M., Hervé, F., Massone, H.-J., Tassinari, C.G., Pankhurst, R., Godoy, E., Theye, T., 2007b. Petrogenesis of the Puerto Edén Igneous and Metamorphic Complex,Magallanes, Chile: Late Jurassic syn-deformational anatexis ofmetapelites and granitoid magma genesis. Lithos, 93, 17-38.

Calderón, M., Prades, C., Hervé, F., Avendaño, V., Fanning, C., Massonne, H., Theye, T., Simonetti, A., 2013. Petrological vestiges of the Late Jurassic-Early Cretaceous transition from rift to back-arc basin in southernmost Chile: New age and geochemical data from the Capitán Aracena, Carlos III, and Tortuga ophiolitic complexes. Geochemical Journal, 47, 201-217.

Carvalho, I., Fernandes, A.C., Andreis, R.R., Paciullo, F.V., Ribeiro, A., Trouw, R.A.J., 2005. The Ichnofossils of the Triassic Hope Bay Formation, Trinity Peninsula Group, Antarctic Peninsula. Ichnos, 12, 191-200.

Castillo, P., Fanning, M.C., Hervé, F., Lacassie, J.P., 2016. Characterization and tracing of Permian magmatism in the south-western segment of the Gondwanan margin; U–Pb age, Lu–Hf and O isotopic compositions of detrital zircons from metasedimentary complexes of northern Antarctic Peninsula and western Patagonia. Gondwana Research, 36, 1-13. https://doi.org/10.1016/j.gr.2015.07.014.

Castillo, P., Fanning, M.C., Pankhurst, R.J., Hervé, F., Rapela, C.W., 2017. Zircon O- and Hf-isotope constraints on the genesis and tectonic significance of Permian magmatism in Patagonia. Journal of the Geological Society, 174, 803-816. https://doi.org/10.1144/jgs2016-152

Cawood, P.A., 2005. Terra Australis Orogen: Rodinia breakup and development of the Pacific and Iapetus margins of Gondwana during the Neoproterozoic and Paleozoic. Earth-Science Reviews, 69, 249-279. http://dx.doi.org/10.1016/j.earscirev.2004.09.001.

Cawood, P.A., Buchan, C., 2007. Linking accretionary orogenesis with supercontinent assembly. Earth-Science Reviews, 69, 249-279. http://dx.doi.org/10.1016/j.earscirev.2004.09.001.

Cawood, P.A., Hawkesworth, C.J., Dhuime, B., 2012. Detrital zircon record and tectonic setting. Geology, 40, 875-878. http://dx.doi.org/10.1130/g32945.1.

Cawood, P.A., Kröner, A., Collins, W.J., Kusky, T.M., Mooney, W.D., Windley, B.F., 2009. Accretionary orogens through Earth history. Geological Society, London, Special Publications, 318, 1-36. https://doi.org/10.1144/SP318.1

Cawood, P.A., Nemchin, A.A., Freeman, M., Sircombre, K., 2003. Linking source and sedimentary basin: Detrital zircon record of sediment flux along a modern river system and implications for provenance studies. Earth and Planetary Science Letters, 210, 1-2, 259-268. https://doi.org/10.1016/S0012-821X(03)00122-5

Chang, Z., Vervoort, J.D., McClelland, W.C., Knaack, C., 2006. U-Pb dating of zircon by LA-ICP-MS. Geochemistry Geophysics Geosystems, 7, 1-14. https://doi.org/10.1029/2005GC001100.

Chemale Jr., F., Ramos, V.A., Naipauer, M., Girelli. T.J., Vargas, M., 2018. Age of basement rocks from the Maurice Ewing Bank and the Falkland/ Malvinas Plateau. Precambrian Research, 314, 28-40. https://doi.org/10.1016/j.precamres.2018.05.026.

640 Cingolani, C.A., Varela, R., 1976. Investigaciones geológicas y geocronologicas en el extremo sur
641 de la isla Gran Malvina, sector de Cabo Belgrano (Cabo Meredith), Islas Malvinas. Actas del
642 sexto Congreso Geologico Argentino 1, 457–73.

643 Collins, W.J., 2002a. Nature of extensional accretionary orogens. Tectonics, 21, 4, 1024.
644 https://doi.org/10.1029/2000TC001272.

645 Collins, W.J., 2002b. Hot orogens, tectonic switching, and creation of continental crust. Geology,
646 30, 6, 535-538. https://doi.org/10.1130/0091-7613(2002)030<0535:HOTSAC>2.0.CO;2.

647 Dalziel, I.W.D., 1981. Back-arc extension in the southern Andes: a review and critical reappraisal.
648 Philosophical Transactions of the Royal Society of London, Series A, 300, 319–335.

649 Dalziel, I.W.D., 1982. The pre-Jurassic history of the Scotia arc: a review and progress report. In:
650 Craddock, C. (Ed.), Antarctic Geoscience. University of Wisconsin Press, 111–126.

651 Del Valle, R.A., Heredia, N., Montes, M., Nozal, F., Martín-Serrano, Á., 2007. El Grupo Trinity
652 Peninsula en la Península Tabarin, extremo norte de la Península Antártica. Revista de la
653 Asociación Geológica Argentina 62, 4, 498-505.

654 Dickinson, W.R., Gehrels, G.E., 2009. Use of U–Pb ages of detrital zircons to infer maximum
655 depositional ages of strata: a test against a Colorado Plateau Mesozoic database. Earth and
656 Planetary Science Letters, 288, 1–2, 115–125.

657 Eagles, G., 2016. Tectonics Reconstructions of the Southernmost Andes and the Scotia Sea during
658 the Opening of the Drake Passage. In: Ghiglione, M.C. (Ed.), Geodynamic Evolution of the
659 Southernmost Andes. Springer Earth System Sciences, 75-108. https://doi.org/10.1007/978-3-
660 319-39727-6_4.

661 Echaurren, A., Oliveros, V., Folguera, A., Ibarra, F., Creixell, C., Lucasse, F., 2016. Early Andean
662 tectonomagmatic stages in north Patagonia: insights from field and geochemical data. Journal of
663 the Geological Society. https://doi.org/10.1144/jgs2016-087.

664 Fang, Z-j., Boucot, A., Covacevich, V., Hervé, F., 1998. Discovery of Late Triassic fossils in the
665 Chonos Metamorphic Complex, Southern Chile. Revista Geológica de Chile, 25, 2, 165-173.

666 Faúndez V., Hervé F., Lacassie J.P., 2002. Provenance studies of pre-late Jurassic metaturbidite
667 successions of the Patagonian Andes, southern Chile. New Zealand Journal of Geology and
668 Geophysics, 45, 4, 411-425.

669 Ferraccioli, F., Jones, P.C., Vaughan, A.P.M., Leat, P.T., 2006. New aerogeophysical view of the
670 Antarctic Peninsula: More pieces, less puzzle. Geophysical Research Letters, 33, L05310.
671 http://doi.org/10.1029/2005GL024636.

672 Forsythe, R.D., Mpodozis, C., 1979. El archipiélago de Madre de Dios, Patagonia Occidental,
673 Magallanes: rasgos generales de la estratigrafía y estructura del basamento pre-Jurásico
674 Superior. Revista Geológica de Chile, 7, 13–29.

675 Forsythe, R.D., Mpodozis, C., 1983. Geología del Basamento pre-Jurásico Superior en el
676 archipiélago Madre de Dios, Magallanes, Chile. Servicio Nacional de Geología y Minería,
677 Boletín 39, 6.

678 Fosdick, J.C., Romans, B.W., Fildani, A., Bernhardt, A., Calderón, M., Graham, S.A., 2001.
679 Kinematic evolution of the Patagonian retroarc fold-and-thrust belt and Magallanes foreland
680 basin, Chile and Argentina, 51°30′S. GSA Bulletin 123, 9-10, 1679-1698. doi:
681 10.1130/B30242.1.

682 Gärtner, A., Linnemann, U., Sagawe, A., Hofmann, M., Ullrich, B., Kleber, A., 2013. Morphology
683 of zircon crystal grains in sediments-characteristics, classifications, definitions. Geologica
684 Saxonica, 59, 65-73.

685 Ghidella, M.E., Lawver, L.A., Marenssi, S., Gahagan, L.M., 2007. Modelos de cinemática de placas
686 para Antártida durante la ruptura de Gondwana: una revisión. Revista de la Asociación
687 Geológica Argentina, 62, 4, 635-645.

688 Ghiglione, M., Likerman, J., Barberón, V., Giambiagi, B., Aguirre-Urreta, B., Suárez, F., 2014.
689 Geodynamic context for the deposition of coarse-grained deep-water axial channel systems in
690 the Patagonian Andes. Basin Research, 1-20. https://doi.org/10.1111/bre.12061.

691 Ghiglione, M., Quinteros, J., Yagupsky, D., Bonillo-Martínez, P., Hlebszevtich, J., Ramos, V.A.,
692 Vergani, G., Figueroa, D., Quesada, S., Zapata, T., 2010. Structure and tectonic history of the
693 foreland basins of southernmost South America. Journal of South American Earth Sciences, 29,
694 262-277. https://doi.org/10.1016/j.jsames.2009.07.006.

695 Ghiglione, M., Ramos, V.A., Cuitiño, J., Barberón, V., 2016. Growth of the Southern Patagonian
696 Andes (46–53°S) and Their Relation to Subduction Processes. In: Folguera A., Naipauer M.,
697 Sagripanti L., Ghiglione M., Orts D., Giambiagi L. (Eds.), Growth of the Southern Andes.
698 Springer Earth System Sciences, 201-240. https://doi.org/10.1007/978-3-319-23060-3_10.

699 Ghiglione, M., Suarez, F., Ambrosio, A., Da Poian, G., Cristallini, E., Pizzio, M., Reinoso, M.,
700 2009. Structure and evolution of the Austral Basin fold-thrust belt, southern Patagonian Andes.
701 Revista Asociación Geológica Argentina, 65, 1, 215-236.

702 Giacosa, R., Fracchia, D., Heredia, N., 2012a. Structure of the Southern Patagonian Andes at 49ºS,
703 Argentina. Geologica Acta 10, 3, 265-282.

704 Giacosa, R., Fracchia, D., Heredia, N., Pereyra, F., 2012b. Hoja Geológica 4972-III y 4975-IV, El
705 Chaltén, provincia de Santa Cruz. Instituto de Geología y Recursos Minerales-Servicio
706 Geológico Minero Argentino. Boletín 399, 86p., Buenos Aires.

707 Giambiagi, L., Tunik, M., Barredo, S., Bechis, F., Ghiglione, M., Alvarez, P., Drosina, M., 2009.
708 Cinemática de apertura del sector norte de la cuenca Neuquina. Revista de la Asociación
709 Geológica Argentina 65, 2, 278-292.

710 Gehrels, G., 2014. Detrital Zircon U-Pb Geochronology Applied to Tectonics. Annual Review of
711 Earth and Planetary Sciences, 42, 127–49. https://doi.org/10.1146/annurev-earth-050212-
712 124012.

Gehrels, G. E., Valencia, V.A., Ruiz, J., 2008. Enhanced precision, accuracy, efficiency, and spatial resolution of U-Pb ages by laser ablation–multicollector–inductively coupled plasma–mass spectrometry. Geochemistry, Geophysics, Geosystems, 9, 3. https://doi.org/10.1029/2007GC001805.

González, J., Oliveros, V., Creixell, C., Velásquez, R., Vásquez, P., Lucassen, F., 2017. The Triassic magmatism and its relation with the Pre-Andean tectonic evolution: Geochemical and petrographic constrains from the High Andes of north central Chile (29° 30'- 30° S). Journal of South American Earth Sciences, in press.

González, P.D., Sato, A.M., Naipauer, M., Varela, R., Basei, M. A. S., Sato, K., Llambías, E.J., Chemale, F., Castro Dorado, A., 2018. Patagonia-Antarctica Early Paleozoic conjugate margins: Cambrian synsedimentary silicic magmatism, U-Pb dating of K-bentonites, and related volcanogenic rocks. Gondwana Research, 63, 186-225.

González, P.D., Sato, A.M., Varela, R., Llambías, E.J., Naipauer, M., Basei, M., Campos, H., Greco, G.A., 2008. El Molino Plutón: A granite with regional metamorphism within El Jagüelito Formation, North Patagonian Massif. In: XI South American Symposium on Isotope Geology. San Carlos de Bariloche, paper 41.

González, P.D., Sato, A.M., Varela, R., Greco, G.A., Naipauer, M., Llambías, E. J., Basei, M. A. S., 2014. Metamorfismo y estructura interna de la Formación El Jagüelito en el Arroyo Salado inferior, Macizo Norpatagónico, Río Negro. In: XIX Congreso Geológico Argentino. Córdoba, 381-382.

González, P.D., Tortello, M.F., Damborenea, S.E., 2011. Early Cambrian Archaeocyathan limestone blocks in low-grade meta-conglomerate from El Jagüelito Formation (Sierra Grande, Río Negro, Argentina). Geológica Acta, 9, 159-173. http://dx.doi.org/10.1344/105.000001650.

González, S.N., Greco, G.A., González, P.D., Sato, A.M., Llambías, E.J., Varela, R., 2016. Geochemistry of a Triassic dyke swarm in the North Patagonian Massif, Argentina. Implications for a postorogenic event of the Permian Gondwanide orogeny. Journal of South American Earth Sciences, 70, 69-82. http://dx.doi.org/10.1016/j.jsames.2016.04.009.

Greco, G.A., González, S.N., Sato, A.M., González, P.D., Basei, M.A.S., Llambías, E.J., Varela, R., 2017. The Nahuel Niyeu basin: a Cambrian forearc basin in the eastern North Patagonian Massif. Journal of South American Earth Sciences, 79, 111-136. http://dx.doi.org/10.1016/j.jsames.2017.07.009.

Harrison, C.G.A., Barron, E.J., Hay, W.W., 1979. Mesozoic evolution of the Antarctic Peninsula and the southern Andes. Geology, 7, 374-378.

Heredia, N., García-Sansegundo, J., Gallastegui, G., Farias, P., Giacosa, R.E., Alonso, J.L., Busquets, P., Charrier, R., Clariana, P., Colombo, F., Cuesta, A., ., Gallastegui, J., Giambiagi, L.B., González-Menéndez, L., Limarino, C.O., Martín-González, F., Méndez-Bedia, I., Pedreira, D., Quintana, L., Rodríguez-Fernández, L.R., Rubio-Ordóñez, A; Seggiaro, R.E., Serra-Varela, S., Spalletti, L.A., Cardó, R., Ramos, V.A., 2016. Evolución geodinámica de los Andes argentinos-chilenos y la Peninsula Antártica durante el Neoproterozico tardío y el Paleozoico. Trabajos de Geología, Universidad de Oviedo, 36, 237-278.

Heredia, N., García-Sansegundo, J., Gallastegui, G., Farias, P., Giacosa, R.E., Hongn, F.D., Tubía, J.M., Alonso, J.L., Busquets, P., Charrier, R., Clariana, P., Colombo, F., Cuesta, A., Gallastegui, J., Giambiagi, L.B., González-Menéndez, L., Limarino, C.O., Martín-González, F., Pedreira, D., Quintana, L., Rodríguez-Fernández, L.R., Rubio-Ordóñez, A; Seggiaro, R.E., Serra-Varela, S., Spalletti, L.A., Cardó, R., Ramos, V.A., 2018. The Pre-Andean phases of construction of the Southern Andes basement in Neoproterozoic-Paleozoic times. In: The Evolution of the Chilean-Argentinean Andes, 111-131. Springer, Cham.

Hervé, F., Nelson, E., Kawashita, K., Suárez, M., 1981a. New isotopic ages and the timing of orogenic events in the Cordillera Darwin, southernmost Chilean Andes. Earth and Planetary Science Letters, 55, 257- 265.

Hervé, F., Mpodozis, C., Davidson, J.A., Godoy, E.P., 1981b. Observaciones estructurales y petrográficas en el basamento metamórfico del archipielago de los Chonos, entre el canal King y el canal Ninualac, Aisen. Revista Geológica de Chile, 13-14, 3-16.

Hervé, F., Calderón, M., Fanning, M., Kraus, S., Pankhurst, R.J., 2010a. SHRIMP chronology of the Magallanes Basin basement, Tierra del Fuego: Cambrian plutonism and Permian high-grade metamorphism. Andean Geology, 37, 2, 253-275.

Hervé, F., Calderón, M., Fanning, M., Pankhurst, R., Fuentes, F., Rapela, C.W., Correa, J., Quezada, P., Marambio, C., 2016. Devonian magmatism in the accretionary complex of southern Chile. Journal of the Geological Society, 173, 587-602. https://doi.org/10.1144/jgs2015-163.

Hervé, F., Calderón, M., Faúndez, V., 2008. The metamorphic complexes of the Patagonian and Fuegian Andes. Geologica Acta, 6, 1, 43-53. http://dx.doi.org/10.1344/105.000000240.

Hervé, F., Fanning, C.M., 2001. Late Triassic zircons in metaturbidites of the Chonos Metamorphic Complex, southern Chile. Revista Geológica de Chile, 28, 1, 91- 104.

Hervé, F., Fanning, C.M., 2003. Early Cretaceous subduction of continental crust at the Diego de Almagro archipelago, southern Chile. Episodes, 26, 4.

Hervé, F., Fanning, C.M., Pankhurst, R.J., 2003. Detrital zircon age patterns and provenance of the metamorphic complexes of southern Chile. Journal of South American Earth Sciences, 16, 107–123. https://doi.org/10.1016/S0895-9811(03)00022-1.

Hervé, F., Fanning, M., Pankhurst, R., Mpodozis, C., Klepeis, K., Calderón, M., Thomson, S.N., 2010b. Detrital zircon SHRIMP U-Pb age study of the Cordillera Darwin Metamorphic Complex of Tierra del Fuego: sedimentary sources and implications for the evolution of the Pacific margin of Gondwana. Journal of the Geological Society, 167, 3, 555-568. https://doi.org/10.1144/0016-76492009-124.

Hervé, F., Miller, H., Pimpirev, C., 2006. Patagonia-Antarctica connections before Gondwana break-up. In: Fütterer, D.K., Dmaske, D., Kleinschmidt, G., Miller, H., Tessensohn, F. (Eds.), Antarctica: Contributions to global earth sciences. Springer-Verlag, 217-227.

789 Hervé, F., Pankhurst, R.J., Fanning, C.M., Calderón, M., Yaxley, G.M., 2007. The South
790 Patagonian batholith: 150 my of granite magmatism on a plate margin. Lithos, 97, 373-394.
791 https://doi.org/10.1016/j.lithos.2007.01.007.

792 Heuret, A., Funiciello, F., Faccenna, C., Lallemand, S., 2007. Plate kinematics, slab shape and
793 back-arc stress: A comparison between laboratory models and current subduction zones. Earth
794 and Planetary Science Letters 256: 473–483.

795 Hyden, G., Tanner, P.W.G., 1981. Late Paleozoic-Early Mesozoic fore-arc basin sedimentary rocks
796 at the Pacific margin in Western Antarctica. Geologische Rundschau, 70, 529–41.

797 Hyppolito, T., Angiboust, S., Juliani, C., Glodny, J., Garcia-Casco, A., Calderón, M.Y Chopin, C.,
798 2016. Eclogite-, amphibolite- and blueschist-facies rocks from Diego de Almagro Island
799 (Patagonia): Episodic accretion and thermal evolution of the Chilean subduction interface during
800 the Cretaceous. Lithos, 264, 422-440. https://doi.org/10.1016/j.lithos.2016.09.001.

801 Jarrad, R.D., 1986. Relations among subduction parameters. Review of Geophysics, 24, 2, 217-284.

802 Jacobs, J., Thomas, R.J., Armstrong, A., Henjes-Kunst, F., 1999. Age and thermal evolution of the
803 Mesoproterozoic Cape Meredith Complex, West Falkland. Journal of the Geological Society,
804 156, 917-928.

805 Jokat, W., Boebel, T., König, M.Y., Meyer, U., 2003. Timing and geometry of early Gondwana
806 breakup. Journal of Geophysical Research, 108, B9, 2428.
807 https://doi.org/10.1029/2002JB001802.

808 Kilian, R., 1990. The Austral Andean Volcanic Zone (South Patagonian), in: International
809 Symposium on Andean Geology, Grenoble, 301-305.

810 Klepeis, K., Betka, P., Clarke, G., Fanning, M., Hervé, F., Rojas, L., Mpodozis, C., Thomson, S.,
811 2010. Continental underthrusting and obduction during the Cretaceous closure of the Rocas
812 Verdes rift basin, Cordillera Darwin, Patagonian Andes. Tectonics, 29, TC3014.
813 https://doi.org/10.1029/2009TC002610.

814 Kobayashi, C., Orihashi, Y., Hiarata, D., Naranjo, J.A., Kobayashi, M., Anma, R., 2010
815 Compositional variations revealed by ASTER image analysis of the Viedma Volcano, southern
816 Andes Volcanic Zone. Andean Geology, 37, 2, 433-441.

817 König, M., Jokat, W., 2006. The Mesozoic breakup of the Weddell Sea. Journal of Geophysical
818 Research-Solid Earth, 111, B12, 1–28.

819 Lacassie, J.P., 2003. Estudio de la Proveniencia Sedimentaria de los Complejos Metamórficos de
820 los Andes Patagónicos (46°- 51° Lat. S), mediante la aplicación de redes neuronales e isótopos
821 estables. Ph.D. thesis, Universidad de Chile, 173pp.

822 Lawver, L.A., Gahagan, L.M., Coffin, M.F., 1992. The development of paleoseaways around
823 Antartica. In: Kennett, J. P., Warnke D. A., (Eds.) The Antarctic Paleoenvironment: A
824 Perspective on Global Change Part 1, A.G.U. Antarctic Research Series, Washington D.C., 56,
825 7-30.

826 Lawver, L.A., Gahagan, L.M., Dalziel, W.D., 1998. A tight fit-early Mesozoic Gondwana, a plate
827 reconstruction perspective. Memoirs of the National Institute for Polar Research, 53, 214–228.

828 Lliboutry, L., 1956. Nieves y glaciares de Chile. Fundamentos de glaciología. Ediciones de la
829 Universidad de Chile, Santiago de Chile.

830 Likerman, J., Burlando, J.F., Cristallini, E., Ghiglione, M., 2013. Along-strike structural variations
831 in the Southern Patagonian Andes: Insights from physical modelling. Tectonophysics, 590, 106-
832 120. https://doi.org/10.1016/j.tecto.2013.01.018.

833 Loske, W., Marquez, M., Giacosa, R., Pezzuchi, H., Fernández, M.I., 1999. U/Pb geochronology of
834 pre-Permian basement rocks in the Macizo del Deseado, Santa Cruz province, Argentine
835 Patagonia. In: XIV Congreso Geológico Argentino. Salta.

836 Ludwig, K.R., 2003. Using Isoplot/Ex, v.3. a Geochronological toolkit for Microsoft Excel.
837 Berkeley Geochronology Center, Special publication, 4.

838 Maloney, K.T., Clarke, G.L., Klepeis, K.A., Fanning, C.M., Wang, W., 2011. Crustal growth during
839 back-arc closure: Cretaceous exhumation history of Cordillera Darwin, southern Patagonia.
840 Journal of Metamorphic Geology, 29, 649–672.

841 Mazzoni, E., Coronato, A., Rabassa, J., 2010. The Southern Patagonian Andes: The Largest
842 Mountain Ice Cap of the Southern Hemisphere. In: Migón, P. (Ed.), Geomorphological
843 Landscapes of the World. Springer Sciences, 12, 111-121. https://doi.org/10.1007/978-90-481-
844 3055-9_12.

845 Millar, I.L., Pankhurst, R.J., Fanning, C.M., 2002. Basement chronology of the Antarctic Peninsula:
846 recurrent magmatism and anatexis in the Palaeozoic Gondwana Margin. Journal of the
847 Geological Society, 159, 145-157. https://doi.org/10.1144/0016-764901-020.

848 Miller, H., 2007. History of views on the relative positions of Antarctica and South America: A
849 100-year tango between Patagonia and the Antarctic Peninsula. USGS Numbered Series, Short
850 Research Paper, 41. https://doi.org/10.3133/ofr20071047SRP041.

851 Miller, H., Loske, W., Kramm, U., 1987. Zircon provenance and Gondwana reconstruction: U-Pb
852 data of detrital zircons from Triassic Trinity Peninsula Formation metasandstones.
853 Polarforschung, 57, 1-2, 59-69.

854 Moreira, P., Fernández, R., Hervé, F., Fanning, C.M., Schalamuk, I.A., 2013. Detrital zircons U-Pb
855 SHRIMP ages and provenance of La Modesta Formation, Patagonia Argentina. Journal of South
856 American Earth Sciences, 47, 32–46. http://dx.doi.org/10.1016/j.jsames.2013.05.010.

857 Naipauer, M., Vujovich, G.I., Cingolani, C.A., McClelland, W.C., 2010. Detrital zircon analysis
858 from the Neoproterozoic–Cambrian sedimentary cover (Cuyania terrane), Sierra de Pie de Palo,
859 Argentina: Evidence of a rift and passive margin system?. Journal of South American Earth
860 Sciences, 29, 306–326.

861 Nelson, J., Gehrels, G., 2007. Detrital zircon geochronology and provenance of the southeastern
862 Yukon-Tanana terrane. Canadian Journal of Earth Sciences, 44, 297-316.

Paces, J., Miller, J., 1993. Precise U-Pb ages of Duluth Complex and related mafic intrusions, northeastern Minnesota; geochronological insights to physical, petrogenetic, paleomagnetic, and tectonomagmatic processes associated with the 1.1 Ga midcontinent rift system. Journal of Geophysical Research, 98, B8, 13997-14013.

Pankhurst, R. J., 1982. Rb-Sr geochronology of Graham Land, Antarctica. Journal of the Geological Society of London, 139, 701-711.

Pankhurst, R.J., Rapela, C.W., Fanning, C.M., Márquez, M., 2006. Gondwanide continental collision and the origin of Patagonia. Earth-Science Reviews, 76, 3−4, 235–257.

Pankhurst, R.J., Rapela, C.W., López de Luchi, M.G., Rapalini, A.E., Fanning, C.M., Galindo, C., 2014. The Gondwana connections of northern Patagonia. Journal of the Geological Society. http://dx.doi.org/10.1144/jgs2013-081.

Pankhurst, R.J., Rapela, C.W., Loske, W.P., Márquez, M., Fanning, C.M., 2003. Chronological study of the pre-Permian basement rocks of southern Patagonia. Journal of South American Earth Sciences, 16, 1, 27–44.

Pankhurst, R.J., Riley, T.R., Fanning, C.M., Kelley, S.P., 2000. Episodic silicic volcanism in Patagonia and the Antarctic Peninsula: chronology of magmatism associated with the break-up of Gondwana. Journal of Petrology, 41, 5, 605–625.

Passchier, C.W., Trouw, R.A.J., 2005. Microtectonics, second ed. Springer-Verlag, Berlín, 366 pp.

Permuy Vidal, C., Moreira, P., Guido, D.M., Fanning, C.M., 2014. Linkages between the southern Patagonia Pre-Permian basements: new insights from detrital zircons U-Pb SHRIMP ages from the Cerro Negro District. Geologica Acta, 12, 2, 137-150.

Ramírez-Sánchez, E., Hervé, F., Kelm, U., Sassi, R., 2005. P-T conditions of metapelites from metamorphic complexes in Aysen, Chile. Journal of South American Earth Sciences, 19, 373-386.

Ramos, V.A., 2008. Patagonia: A Paleozoic continent adrift? Journal of South American Earth Sciences, 26, 235-251. http://dx.doi.org/10.1016/j.jsames.2008.06.002.

Ramos, V.A., 2010. The tectonic regime along the Andes: Present-day and Mesozoic regimes. Geological Journal, 45, 2-25. DOI: 10.1002/gj.1193.

Ramos, V.A., Cingolani, C., Chemale Jr., F., Naipauer, M., Rapallini, A., 2017. The Malvinas (Falkland) Islands revisited: The tectonic evolution of southern Gondwana based on U-Pb and Lu-Hf detrital zircon isotopes in the Paleozoic cover. Journal of South American Earth Sciences, 76, 320-345. http://dx.doi.org/10.1016/j.jsames.2016.12.013.

Rapalini, A.E., Hervé. F., Ramos, V.A., Singer, S.E., 2001. Paleomagnetic evidence for a very large counterclockwise rotation of the Madre de Dios Archipelago, southern Chile. Earth and Planetary Science Letters, 184, 471-478. https://doi.org/10.1016/S0012-821X(00)00339-3.

Rapalini, A.E., López de Luchi, M., Tohver, E., Cawood, P.A., 2013. The South American ancestry of the North Patagonian Massif: geochronological evidence for an autochthonous origin? Terra Nova, 25, 337-342. http://dx.doi.org/10.1111/ter.12043.

Rapela, C.W., Pankhurst, R.J., Harrison, S.M., 1992. Triassic "Gondwana" granites of the Gastre district, North Patagonian Massif. Transactions of the Royal Society of Edinburgh: Earth Sciences, 83, 291-304.

Rex, D.C., Tanner, P.W.G., 1982. Precambrian ages for gneisses at Cape Meredith in the Falkland Islands. In: Craddock, C. (Ed.), Antarctic Geoscience. University of Wisconsin Press, 107-110.

Riley, T. R., Flowerdew, M. J., Pankhurst, R. J., Curtis, M. L., Millar, I. L., Fanning, M. C., Whitehouse, M. J., 2016. Early Jurassic magmatism on the Antarctic Peninsula and potential correlation with the Subcordilleran plutonic belt of Patagonia. Journal of the Geological Society, 174, 365-376. https://doi.org/10.1144/jgs2016-053.

Riley, T.R., Flowerdew, M.J., Whitehouse, M.J., 2012. U–Pb ion-microprobe zircon geochronology from the basement inliers of eastern Graham Land, Antarctic Peninsula. Journal of the Geological Society, 169, 4, 381–393.

Riley, T.R., Leat, P.T., Pankhurst, R.J., Harris, C., 2001. Origins of large volume rhyolitic volcanism in the Antarctic Peninsula and Patagonia by crustal melting. Journal of Petrology, 42, 6, 1043-1065. https://doi.org/10.1093/petrology/42.6.1043.

Riley, T.R., Flowerdew, M.J., Hunter, M.A., Whitehouse, M.J., 2010. Middle Jurassic rhyolite volcanism of eastern Graham Land, Antarctic Peninsula: age correlations and stratigraphic relationships. Geological Magazyne, 147, 4, 581-595. https://doi.org/10.1017/S0016756809990720.

Saini-Eidukat, B., Beard, B., Bjerg, E.A., Gehrels, G., Gregori, D., Johnson, C., Migueles, N., Vervoort, J.D., 2004. Rb-Sr and U-Pb age systematics of the Alessandrini silicic complex and related mylonites, Patagonia, Argentina. In: Geological Society of America, Denver Annual Meeting. Denver, paper 88-14.

Schiffman, P., Day, H.W., 1999. Petrological methods for the study of very low-grade metabasites. In: Frey, M., Robinson, D. (Eds.), Low-Grade Metamorphism. Blackwell Science, 108-141.

Schilling, M.E., Carlson, R.W., Tassara, A., Conceição, R.V., Bertotto, G.W., Vázquez, M., Muñoz, D., Jalowitzki, T., Gervasoni, F., Morata, D., 2017. The origin of Patagonia revealed by Re-Os systematics of mantle xenoliths. Precambrian Research, 294, 15-32. http://dx.doi.org/10.1016/j.precamres.2017.03.008.

Serra-Varela, S., Giacosa, R., González, P., Heredia, N., Martín-González, F., Pedreira, D., 2016. Geología y geocronología del basamento paleozoico de los Andes Norpatagónicos en el área de San Martín de los Andes, In: IX Congreso Geológico de España, GEO-TEMAS. Huelva, 16, 431-434.

Shipton, E., 1960. Volcanic activity on the Patagonian Ice Cap. Geographical Journal, 126, 4, 389-396.

936 Shipton, E., 1963. Land of Tempest: Travels in Patagonia 1958-1962, first ed. Hodder and
937 Stoughton, 222 pp.

938 Sláma, J., Kosler, J., Condon, D.J., Crowley, J.L., Gerdes, A., Hanchar, J.M., Horstwood, M.S.A.,
939 Morris, G.A., Nasdala, L., Norberg, N., Schaltegger, U., Schoene, B., Tubrett, M.N.,
940 Whitehouse, M.J., 2008. Plesovice zircon - a new natural reference material for U-Pb and Hf
941 isotopic microanalysis. Chemical Geology, 249, 1-35.

942 Söllner, F., Miller, H., Hervé, M., 2000. An Early Cambrian granodiorite age from the pre-Andean
943 basement of Tierra del Fuego (Chile): the missing link between South America and Antarctica?.
944 Journal of South American Earth Sciences, 13, 163–177. https://doi.org/10.1016/S0895-
945 9811(00)00020-1.

946 Spencer, C.J., Kirkland, C.L., Taylor, R.J.M., 2016. Strategies towards statistically robust
947 interpretations of in situ U-Pb zircon geochronology. Geoscience Frontiers, 7, 581-589.
948 http://dx.doi.org/10.1016/j.gsf.2015.11.006.

949 Spikings, R., Reitsma, M.J., Boekhout, F., Mišković, A., Ulianov, A., Chiaradia, M., Gerdes, A.,
950 Schategger, U., 2016. Characterisation of Triassic rifting in Peru and implications for the early
951 disassembly of western Pangaea. Gondwana Research 35, 124-143.

952 Stern, R.J., 2002. Subduction zones. Review of Geophysics 40, 4, 1012,
953 doi:10.1029/2001RG000108.

954 Stern, C.R., de Wit, M.J., 2003. Rocas Verdes ophiolites, southernmost South America: remnants of
955 progressive stages of development on oceanic-type crust in a continental margin back-arc basin.
956 In: Dilek, Y., Robinson, P.T. (Eds.), Ophiolites in Earth History. Geological Society, Special
957 Publications, 1–19.

958 Suárez, M., 1976. Plate-tectonic model for southern Antarctic Peninsula and its relation to southern
959 Andes. Geology, 4, 211-214. https://doi.org/10.1130/0091-
960 7613(1976)4<211:PMFSAP>2.0.CO;2.

961 Tera, F., Wasserburg, G.J., 1972. U-Th-Bb systematics in three Apollo 14 basalts and the problem
962 of initial Pb in lunar rocks. Earth and Planetary Science Letters, 14, 281-304.

963 Thomas, R.J., Jacobs, J., Eglintong, B.M., 2000. Geochemistry and isotopic evolution of the
964 Mesoproterozoic Cape Meredith Complex, West Falkland. Geological Magazine, 137, 5, 537-
965 553.

966 Thomson, S.N., Hervé, F., 2002. New time constraints for the age of metamorphism at the ancestral
967 Pacific Gondwana margin of souther Chile (42-52°S). Revista Geológica de Chile, 28, 2, 255-
968 271.

969 Trouw, R.A.J., Passchier, C.W., Simões, L.S.A., Andreis, R.R., Valerianos, C.M., 1997. Mesozoic
970 tectonic evolution of the South Orkney Microcontinent, Scotia Arc, Antarctica. Geological
971 Magazine, 134, 3, 383-401.

Uyeda, S., Kanamori, H., 1979. Back-arc opening and the mode of subduction. Journal of Geophysical Research 84, 3, 1049-1061.

Varela, R., Basei, M.A.S., Cingolani, C.A., Siga Jr., O., Passarelli, C. R., 2005. El basamento cristalino de los Andes norpatagónicos en Argentina: geocronología e interpretación tectónica. Revista Geológica de Chile, 32, 2, 167-187.

Vaughan, A.P.M., Livermore, R.A., 2005. Episodicity of Mesozoic terrane accretion along the Pacific margin of Gondwana: implications for superplume-plate interactions. In: Vaughan, A.P.M., Leat, P.T., Pankhurst, R.J. (Eds.), Terrane Processes at the Margins of Gondwana. Geological Society, Special Publications, 1-21.

Vaughan, A.P.M., Storey, B.C., 2000. The eastern Palmer Land shear zone: A new terrane accretion model for the Mesozoic development of the Antarctic Peninsula. Journal of the Geological Society, 157, 1243-1256. http://doi.org/10.1144/jgs.157.6.1243.

Vaughan, A.P.M., Eagles, G., Flowerdew, M.J., 2012. Evidence for a two-phase Palmer Land event from crosscutting structural relationships and emplacement timing of the Lassiter Coast Intrusive Suite, Antarctic Peninsula: Implications for mid-Cretaceous Southern Ocean plate configuration. Tectonics, 31, TC1010.

Wareham, C.D., Pankhurst, R.J., Thomas, R.J., Storey, B.C., Grantham, G.H., Jacobs, J., Eglington, B.M., 1998. Pb, Nd, and Sr Isotope Mapping of Grenville-Age Crustal Provinces in Rodinia. The Journal of Geology, 106, 647-659. https://doi.org/10.1086/516051.

Wetherill, G.W., 1956. Discordant uranium-lead ages, I. Transactions, American Geophysical Union, 37, 3, 320-326. http://dx.doi.org/10.1029/TR037i003p00320.

Wever, H.E., Millar, I.L., Pankhurst, R.J., 1994. Geochronology and radiogenic isotope geology of Mesozoic rocks from eastern Palmer Land, Antarctic Peninsula: crustal anatexis in arc-related granitoid genesis. Journal of South American Earth Sciences, 7, 1, 69-83.

Willan, R.C.R., Pankhurst, R.J., Hervé, F., 1994. A probable Early Triassic age for the Miers Bluff Formation, Livingston Island, South Shetland Islands. Antarctic Science, 6, 3, 401-408.

Willner, A., Hervé, F., Massonne, H.J., 2000. Mineral chemistry and pressure-temperature evolution of two contrasting high-pressure-low-temperature belts in the Chonos Archipelago, Southern Chile. Journal of Petrology, 41, 3, 309-330. https://doi.org/10.1093/petrology/41.3.309.

Willner, A.P., Sepúlveda, F.A., Hervé, F., Massonne, H-J., Sudo, M., 2009. Conditions and timing of pumpellyite–actinolite-facies metamorphism in the Early Mesozoic frontal accretionary prism of the Madre de Dios Archipelago (Latitude 50°20′S; Southern Chile). Journal of Petrology, 50, 2127–2155. https://doi.org/10.1093/petrology/egp071.

Williams, I.S., 1998. U-Th-Pb geochronology by ion microprobe. Reviews in Economic Geology, 7, 1-35.

1007 Zaffarana, C.B., Somoza, R., López de Luchi, M., 2014. The Late Triassic Central Patagonian
1008 Batholith: Magma hybridization, 40Ar/39Ar ages and thermobarometry. Journal of South
1009 American Earth Sciences, 55, 94-122. http://dx.doi.org/10.1016/j.jsames.2014.06.006.

1010 Zaffarana, C.B., Somoza, R., Orts, D.L., Mercader, R., Boltshauser, B., González, V.R.,
1011 Puigdomenech, C., 2017. Internal structure of the Late Triassic Central Patagonian batholith at
1012 Gastre, southern Argentina: Implications for pluton emplacement and the Gastre fault system.
1013 Geosphere 13, 6. doi:10.1130/GES01493.1.

1014 Zerfass, H., Ramos, V. A., Ghiglione, M. C., Naipauer, M., Belotti, H. J., & Carmo, I. O. 2017.
1015 Folding, thrusting and development of push-up structures during the Miocene tectonic inversion
1016 of the Austral Basin, Southern Patagonian Andes (50° S). Tectonophysics 699, 102-120.

1017 **FIGURE CAPTIONS**

1018 Figure 1. (a) Location and geological map of the study area (modified from Giacosa et al.,
1019 2012b). The yellow star corresponds to the U-Pb detrital zircons sampling site. (b) Zoom-in
1020 on the Nunatak Viedma-Paso del Viento showing with major precision the sample site.

1021 Figure 2. Paleogeographic reconstruction of Pangea at 200 Ma (Triassic-Jurassic boundary)
1022 showing the relative position between Patagonia and Antarctic Peninsula (modified from
1023 the "tight fit model" by Lawver et al., 1998).

1024 Figure 3. Pre-Jurassic representative ages from Patagonia and Antarctic Peninsula. CMC:
1025 Chonos Metamorphic Complex; CPB: Central Patagonian Batholith; CPVC: Curaco
1026 Plutonic-Volcanic Complex. DMC: Darwin Metamorphic Complex; EAMC: Eastern Andes
1027 Metamorphic Complex; MDAC: Madre de Dios Accretionary Complex; NPA: North
1028 Patagonian Andes. NVM: Nunatak Viedma Metamorphites. SOI: South Orkney Islands.
1029 SPA: Southern Patagonian Andes. Patagonian ages are from Saini-Eidukat et al. (2004),
1030 Pankhurst et al. (2006), Zaffarana et al. (2014) and Greco et al. (2017) in the North
1031 Patagonian Massif; Pankhurst et al. (2003, 2006), Moreira et al. (2013) and Permuy Vidal
1032 et al. (2014) in the Deseado Massif; Cingolani and Varela (1976) and Jacobs et al. (1999) at
1033 Malvinas Islands; Hervé and Fanning (2001), Varela et al. (2005), Pankhurst et al. (2006),
1034 Hervé et al. (2016) and Serra-Varela et al. (2016) in the Northern Patagonian Andes and
1035 North Patagonian Chilean coast; Hervé et al. (2003) in the Southern Patagonian Andes;
1036 Sölner et al. (2000), Barbeau et al. (2009b), Calderón et al. (2010), Hervé et al. (2010) and
1037 Castillo et al. (2017) in the Fuegian Andes. Antarctic Peninsula´s ages are from Pankhurst
1038 (1982), Willan et al. (1994), Millar et al. (2002), and Riley et al. (2012).

1039 Figure 4. LA-ICP-MS U-Pb zircon ages for MN-0, MN-1 and MN-10 samples plotted in
1040 Tera and Wasserburg (1972) concordia diagrams. The left column corresponds to the entire
1041 spectrum of ages while the right column shows principally Paleozoic ages.

1042 Figure 5. The left column corresponds to the frequency histograms and relative probability
1043 plots of U-Pb detrital zircon ages (LA-ICP-MS). The inset shows weighted average age
1044 plots of the youngest cluster overlapping at 1σ. Weighted mean age is interpreted as the

maximum depositional age. Pie-chart with the distribution of the zircon detrital ages for each sample is represented on the right column.

Figure 6. Outcrops of the Nunatak Viedma locality showing lithological and structural features. A) Very low-grade metapsammites and metapelites with excellent preservation of bedding cut by a mid angle reverse fault. B) Metasedimentary rocks interbedded with metabasites with boudins development and calcite veins in the neck of the structure. S1 dip/dip direction is 60°/340°. C) Metapsammites and metapelites showing upright isoclinal and tight folds, and high-angle reverse faults.

Figure 7. Photomicrographs of metapsammites and metabasites from NVU. A) typical composition of the metapsammites. B) S_1 cleavage and associated growth of chlorite + sericite. C) S_1 cleavage affected by a crenulation cleavage (S_2) developed in brittle conditions. D) Metabasite with porphyric texture exhibiting plagioclases + clinopyroxene phenocrysts within fine-grained groundmass composed by mafites, opaques, and plagioclase.

Figure 8. Paleozoic-lower Mesozoic relative probability distribution from Chonos Metamorphic Complex (CE9603, FO9606 and CE9625 samples from Hervé and Fanning, 2001) and Viedma Nunatak Unit (MN0, MN10 and MN1 samples from this study). NVU shows prominent lower Paleozoic peaks, which are not represented in the CMC, while the Permian-Triassic peaks are represented in both units. Violet and sky-blue lines depict the MDA from CMC and NVU, respectively.

Figure 9. Samples from the Chonos Metamorphic Complex and the Nunatak Viedma Unit are plotted as curves of cumulative proportion based on differences between the crystallization and depositional ages (CA – DA) of the detrital zircons. This diagram enabling prediction of the tectonic setting of metasedimentary packages of unknown origin (see procedure in Cawood et al., 2012). Both metamorphic units present typical curves of convergent setting while the Chonos Metamorphic Complex presents a typical curve for forearc or trench basins, the Nunatak Viedma Unit presents a curve akin to backarc basins. Brown areas represent overlapping tectonic fields.

Figure 10. Interpretation of the Late Triassic tectonic setting of the southwestern margin of Pangea and the paleogeographic implications on the Patagonia-Antarctic Peninsula connection. The A-A' schematic profile exhibits the tectonic setting south of the 47°S, and the developed of the Nunatak Viedma basin in a retroarc postion respect to the magmatic arc emplaced along Antarctic Peninsula. Subsequent closure of the basin ocurred during the Chonide deformation event. The B-B' schematic profile (based from Rapela et al., 1992; Zaffarana et al., 2014, 2017) show the tectonic setting north of the 47°S. The red line in the paleogeographic reconstruction depicts the position of the magmatic arc (topographic barrier) emplaced along Antarctic Peninsula arc with continuation in Patagonia (Central Patagonian Batholith and farther north). EAMC: Eastern Andes Metamorphic Complex. GSF: Greywacke-Shale Formation.

Figure 11. Correlation between units from Patagonia and Antarctic Peninsula and the tectonic events happened during the early Mesozoic in the southwestern margin of Pangea. Besides, we exhibit representative geochemical features of the volcanic and plutonic units. Based on Dalziel (1982), Trouw et al. (1997), Thomson and Hervé (2002), König y Jokat (2006), Calderón et al. (2007, 2013), Hervé et al. (2007), Riley et al. (2010), Vaughan et al. (2012), Zaffarana et al. (2014), Echaurren et al. (2016), Ghiglione et al. (2016) and this study. V1, V2, and V3 represent episodes of Jurassic volcanism defined by Pankhurst et al. (2000).

APPENDIX A. SUPPLEMENTARY DATA.

Table A. LA-ICPMS U-Pb geochronological analyses in detrital zircons of the samples MN-0, MN-1, and MN-10.

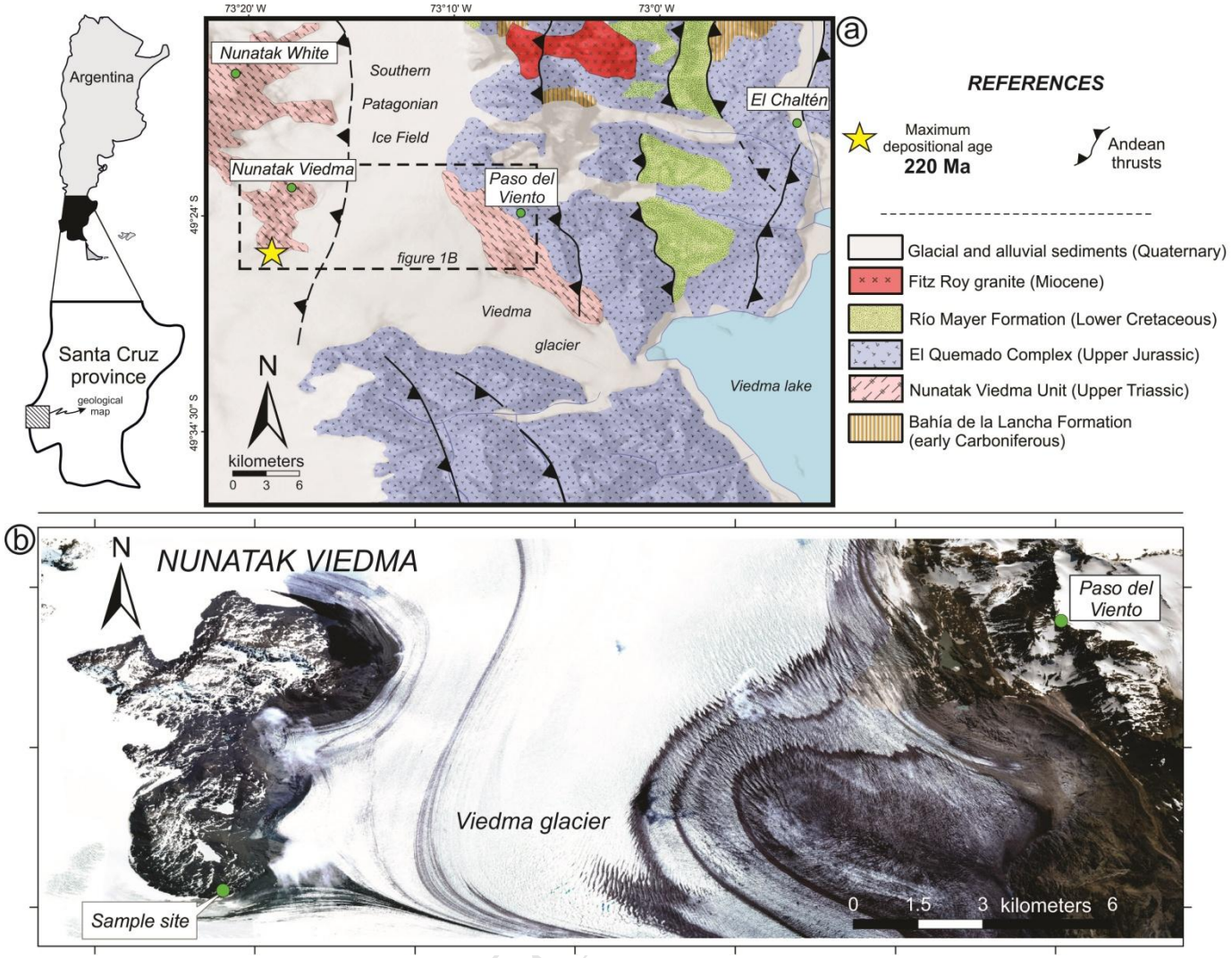

FIGURE 1

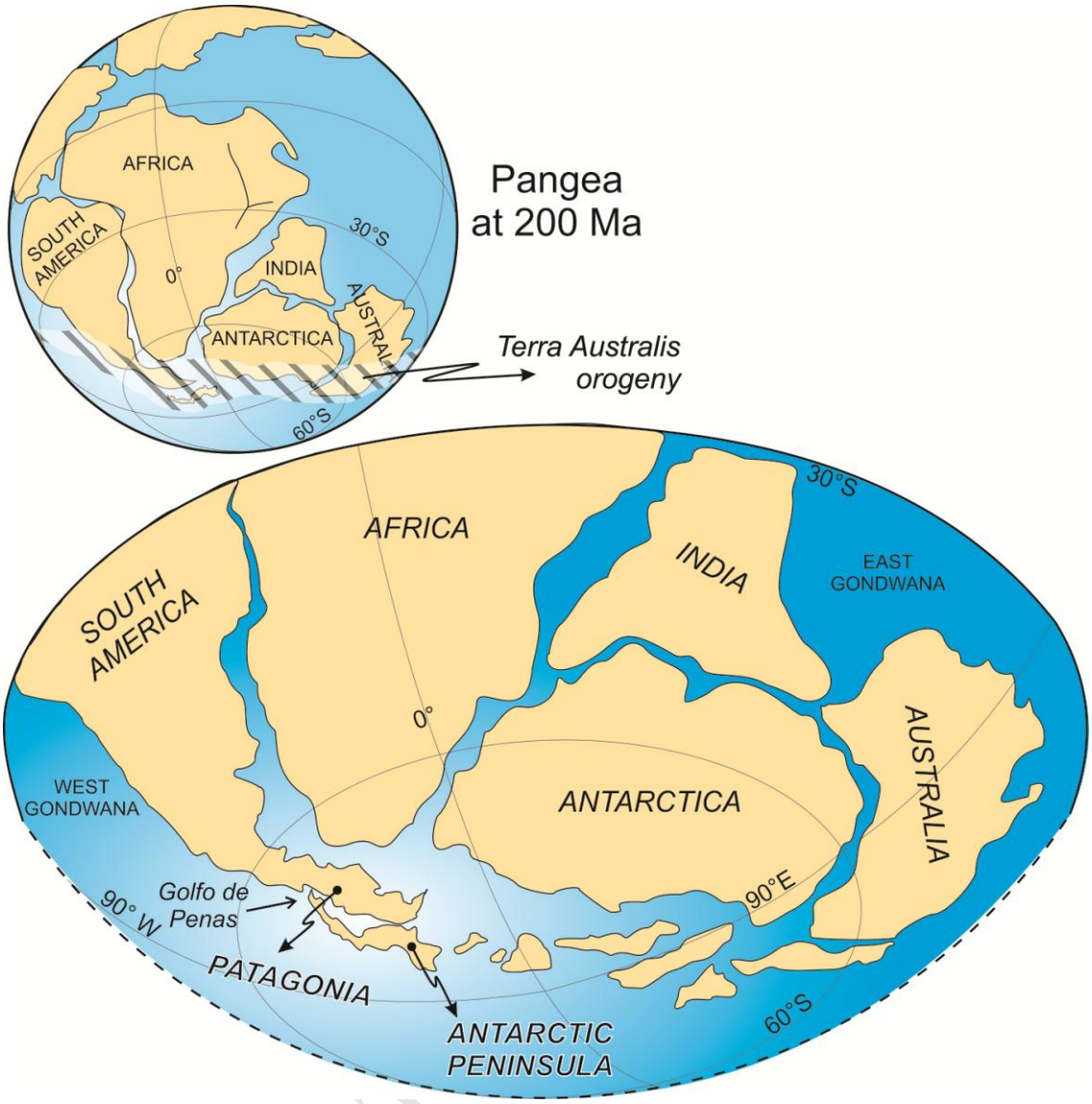

FIGURE 2

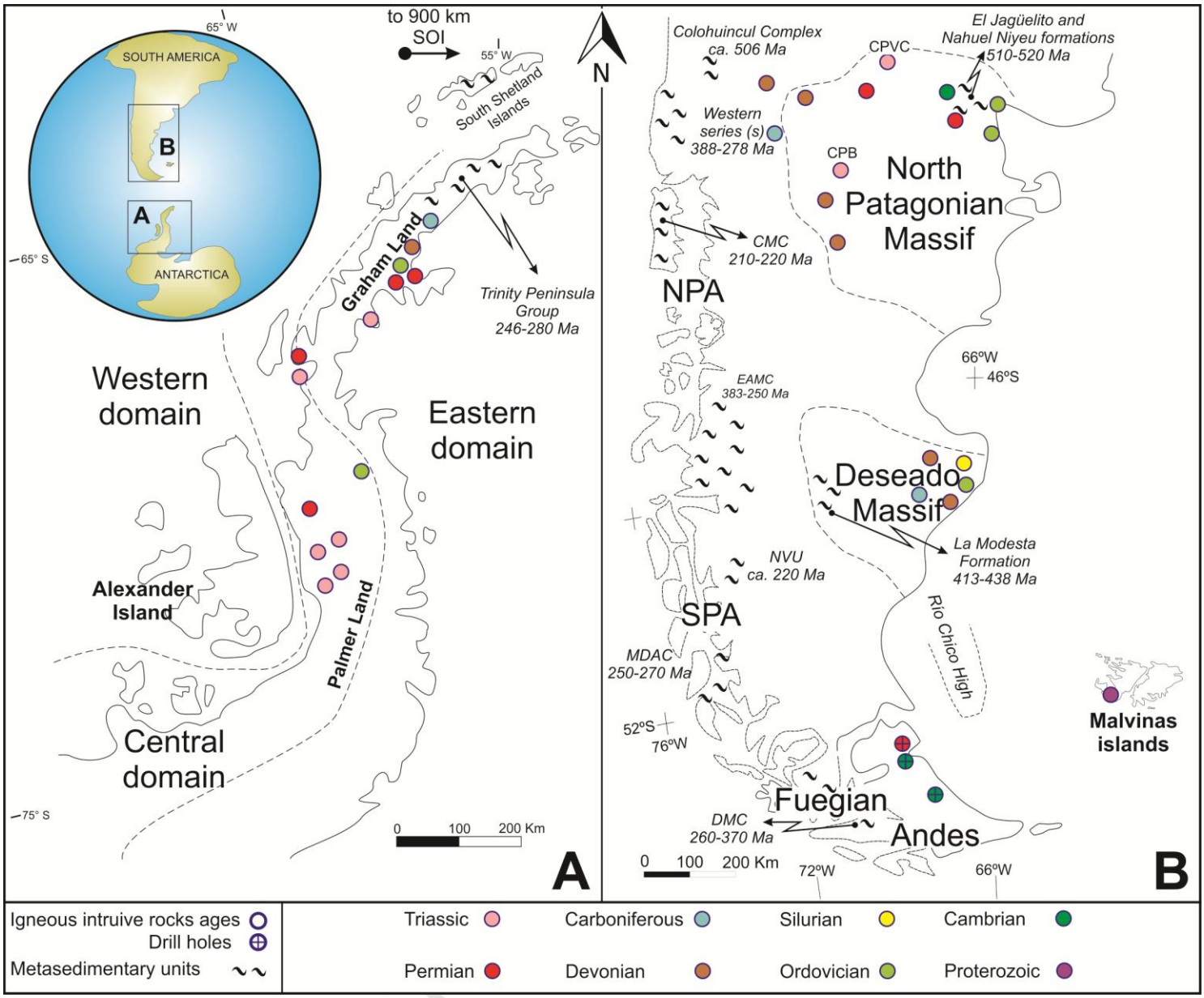

FIGURE 3

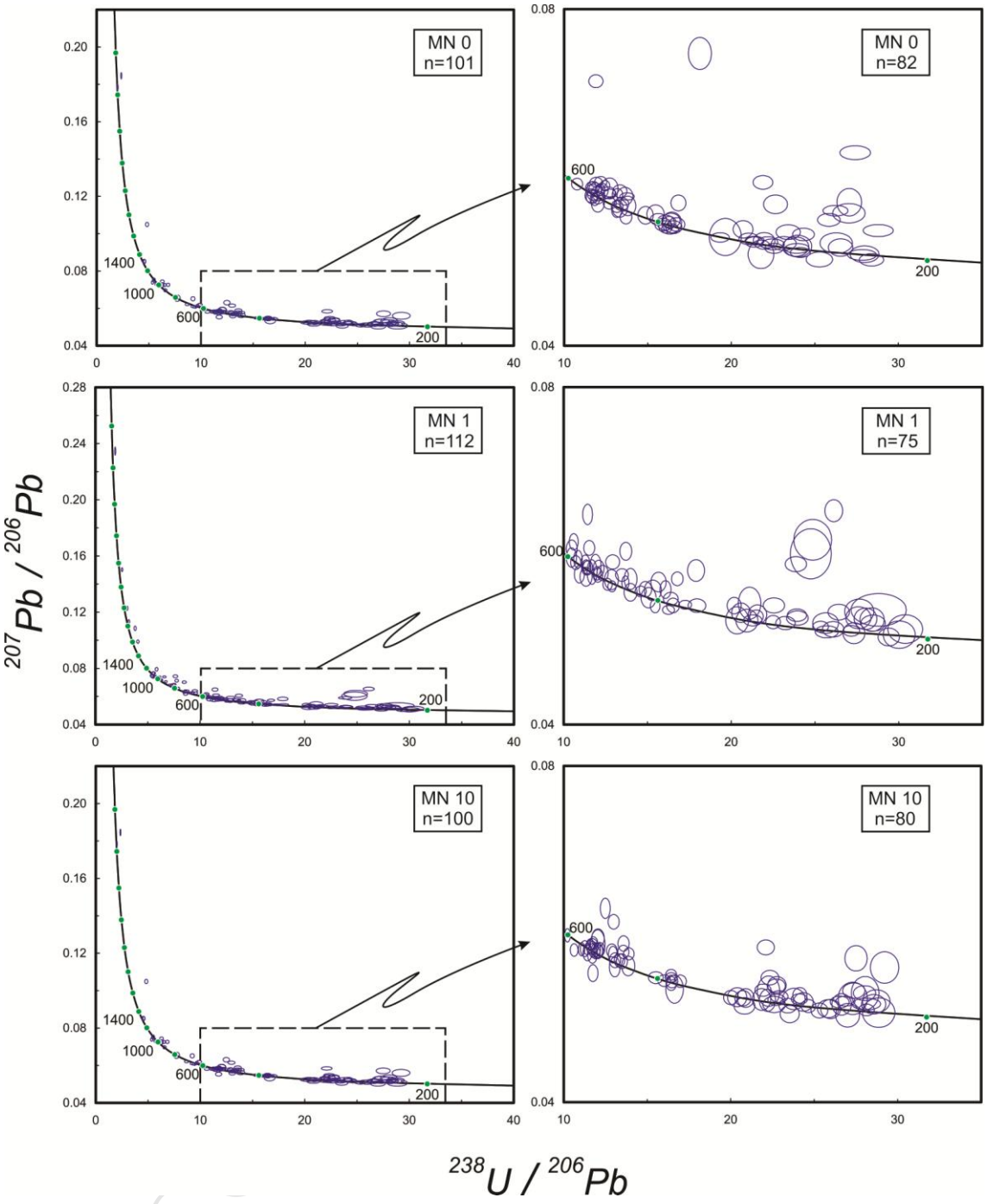
MN 0
n=101
MN 0
n=82
MN 1
n=112
MN 1
n=75
MN 10
n=100
MN 10
n=80
1400
1000
600
200
$^{207}Pb / ^{206}Pb$
$^{238}U / ^{206}Pb$

FIGURE 4

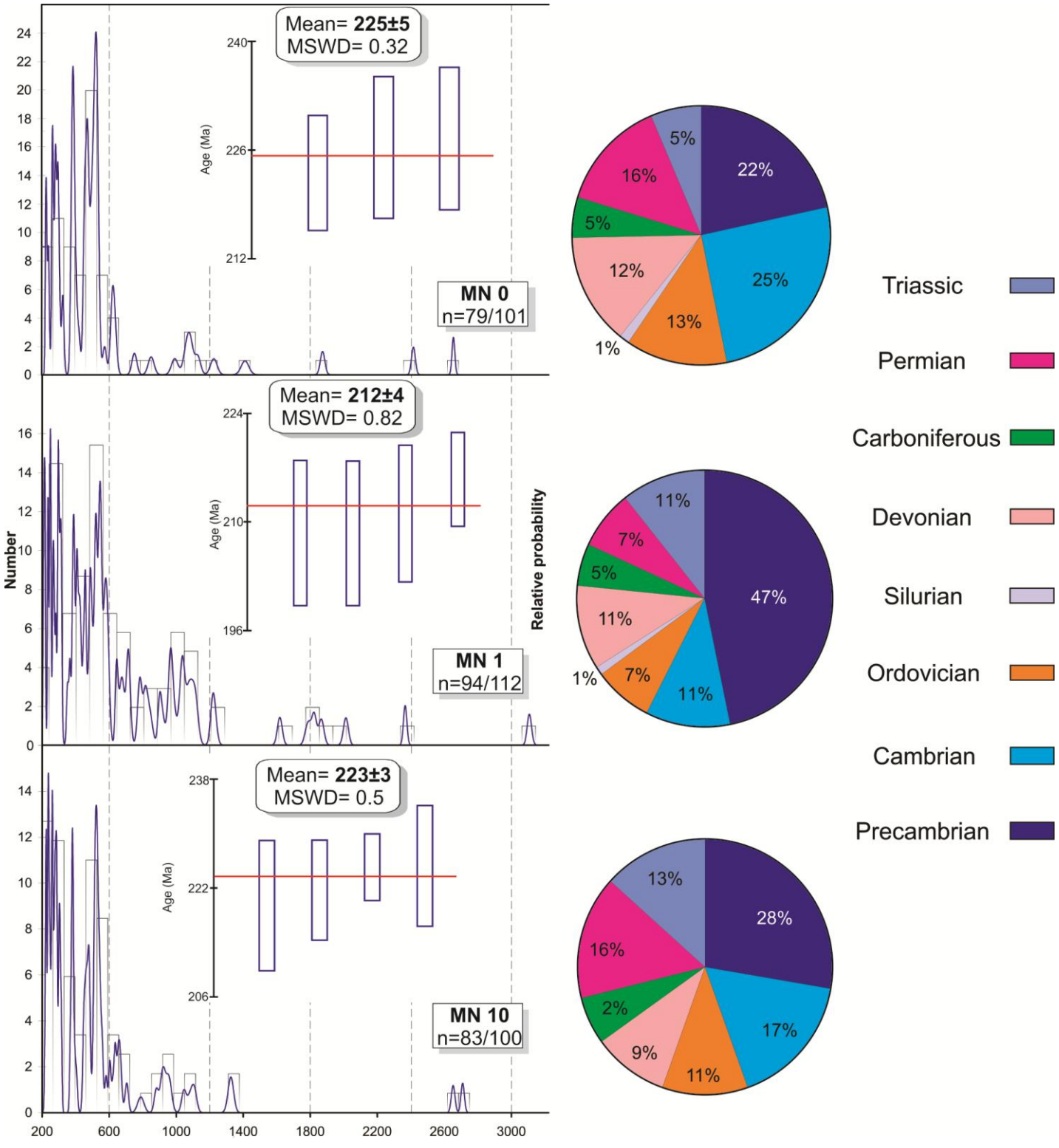
Mean= 225±5
MSWD= 0.32
MN 0
n=79/101
Mean= 212±4
MSWD= 0.82
MN 1
n=94/112
Mean= 223±3
MSWD= 0.5
MN 10
n=83/100
Age (Ma)
Number
Relative probability
5%
22%
16%
5%
12%
25%
13%
1%
11%
7%
5%
47%
11%
1%
7%
11%
13%
28%
16%
2%
17%
9%
11%
Triassic
Permian
Carboniferous
Devonian
Silurian
Ordovician
Cambrian
Precambrian

FIGURE 5

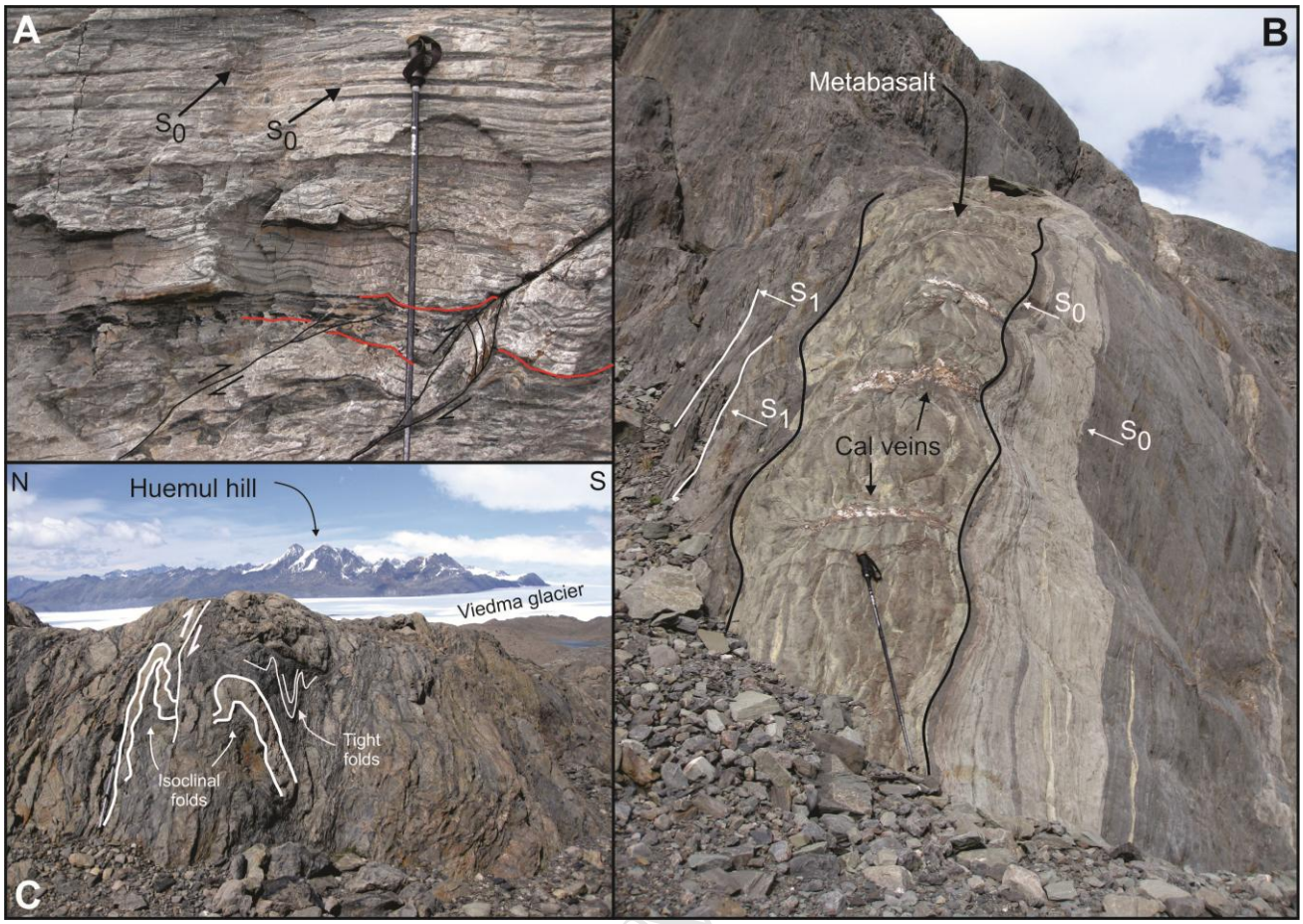

FIGURE 6

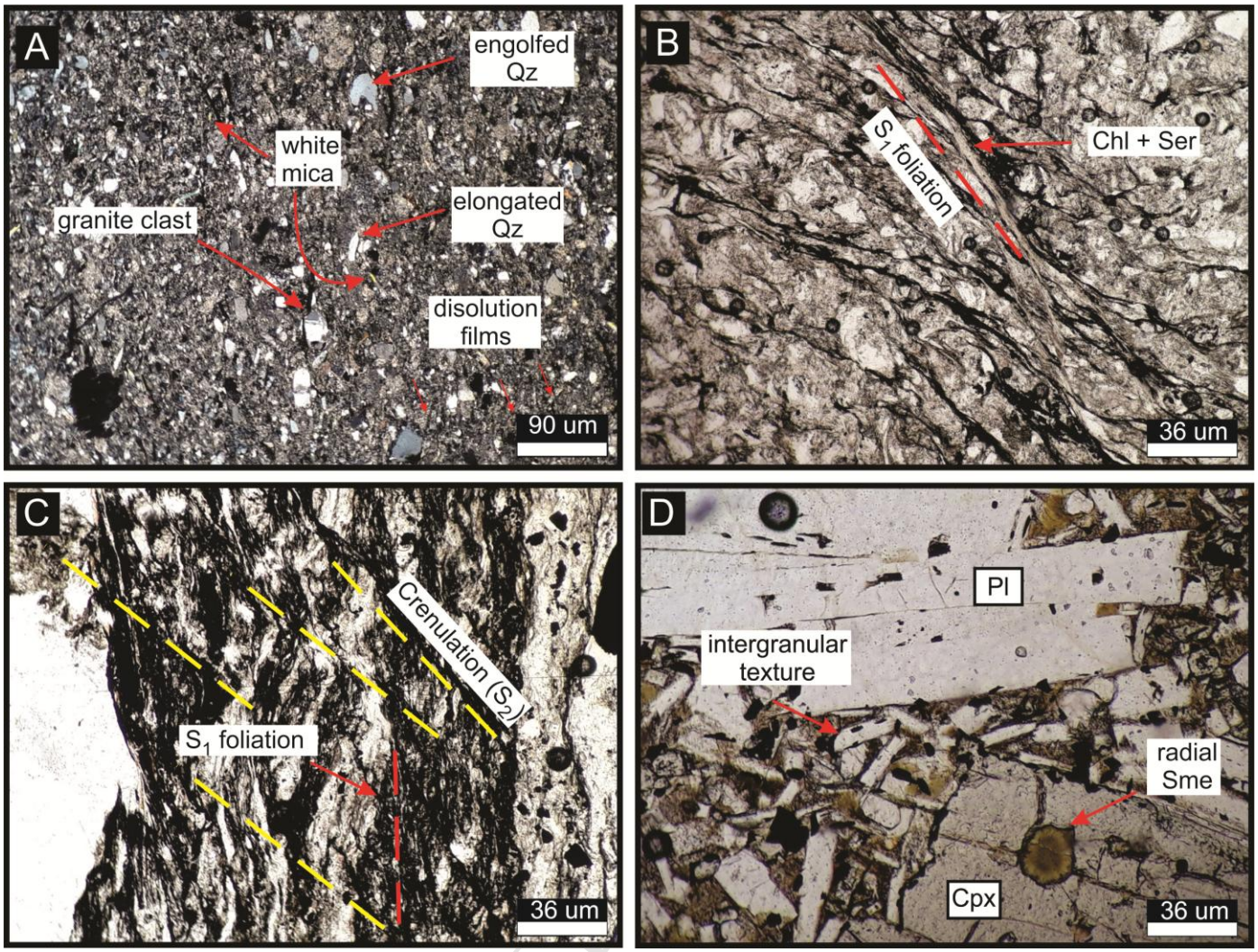

FIGURE 7

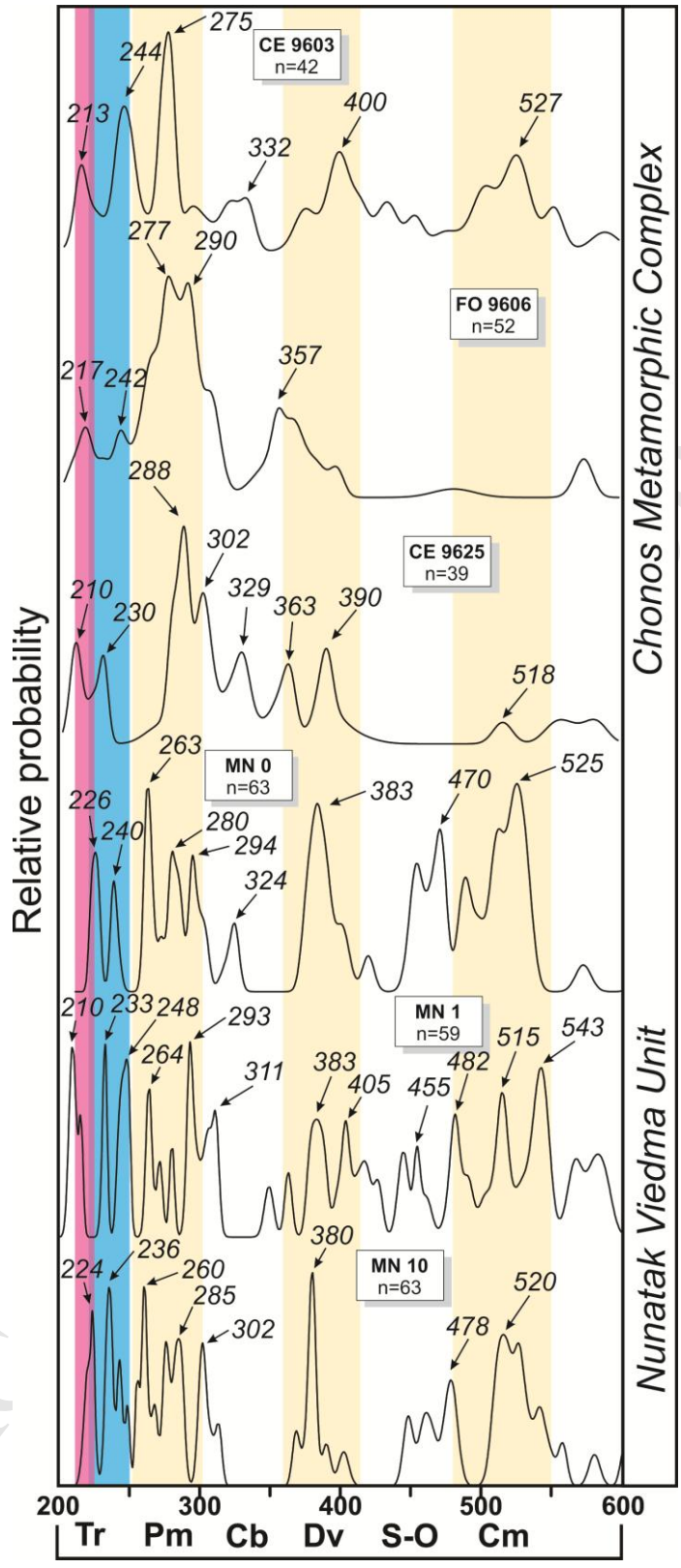
CE 9603
n=42
275
244
213
400
527
332
277
290
FO 9606
n=52
357
217
242
288
CE 9625
n=39
302
210
230
329
363
390
518
MN 0
n=63
263
226
240
280
294
324
383
470
525
MN 1
n=59
210
233
248
293
264
311
383
405
455
482
515
543
MN 10
n=63
224
236
260
285
302
380
478
520
Relative probability
Chonos Metamorphic Complex
Nunatak Viedma Unit
200
300
400
500
600
Tr
Pm
Cb
Dv
S-O
Cm

FIGURE 8

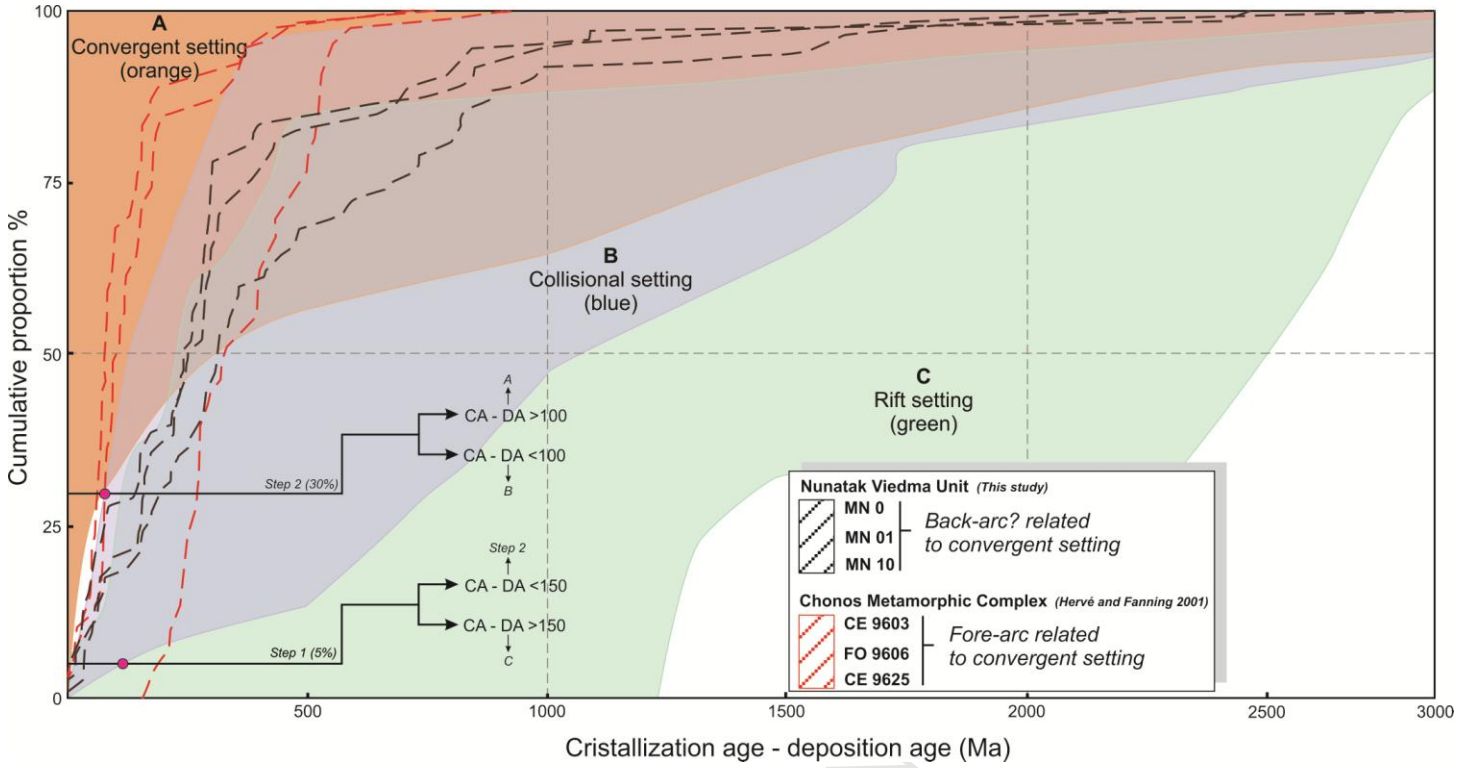

FIGURE 9

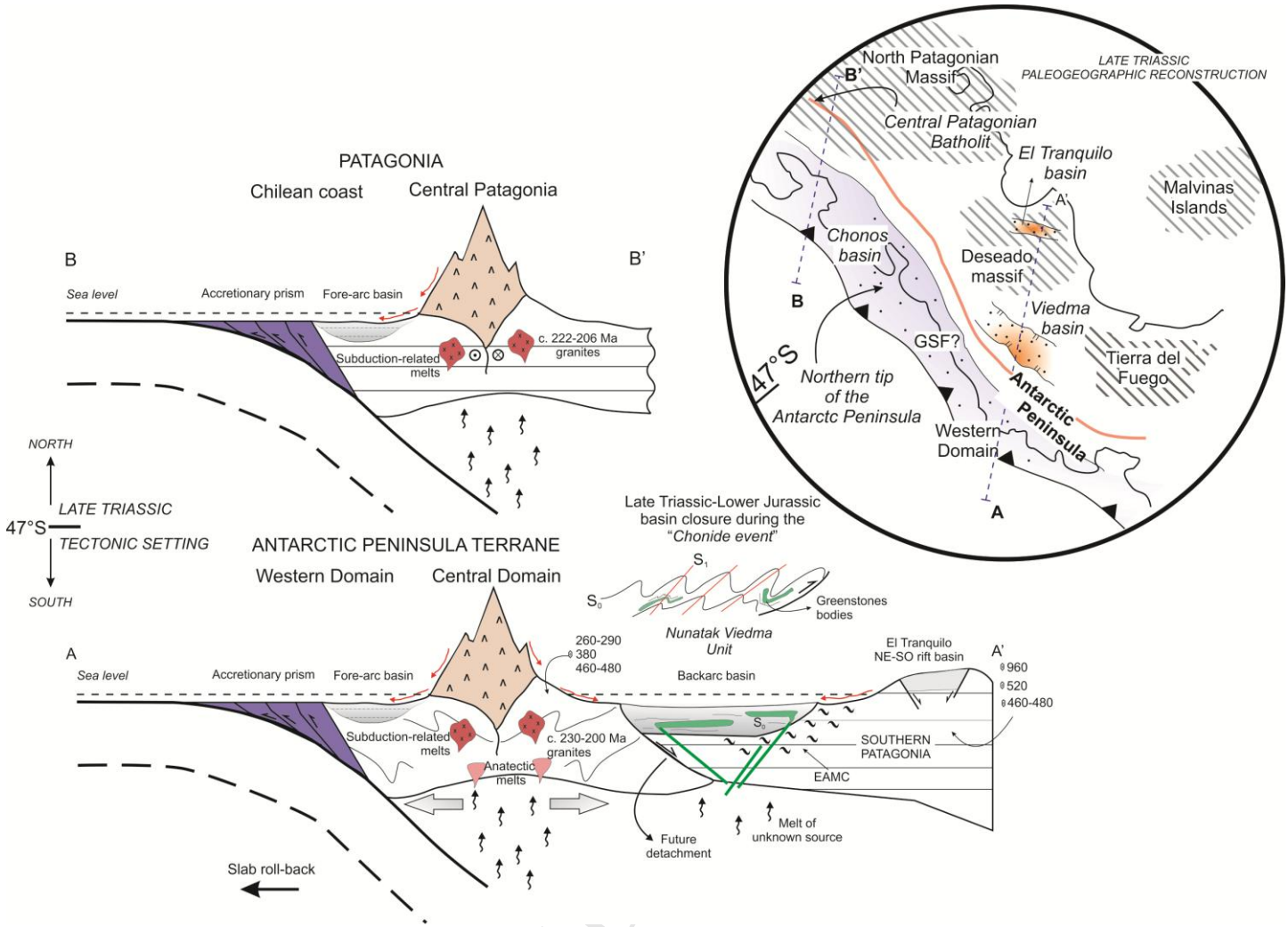

FIGURE 10

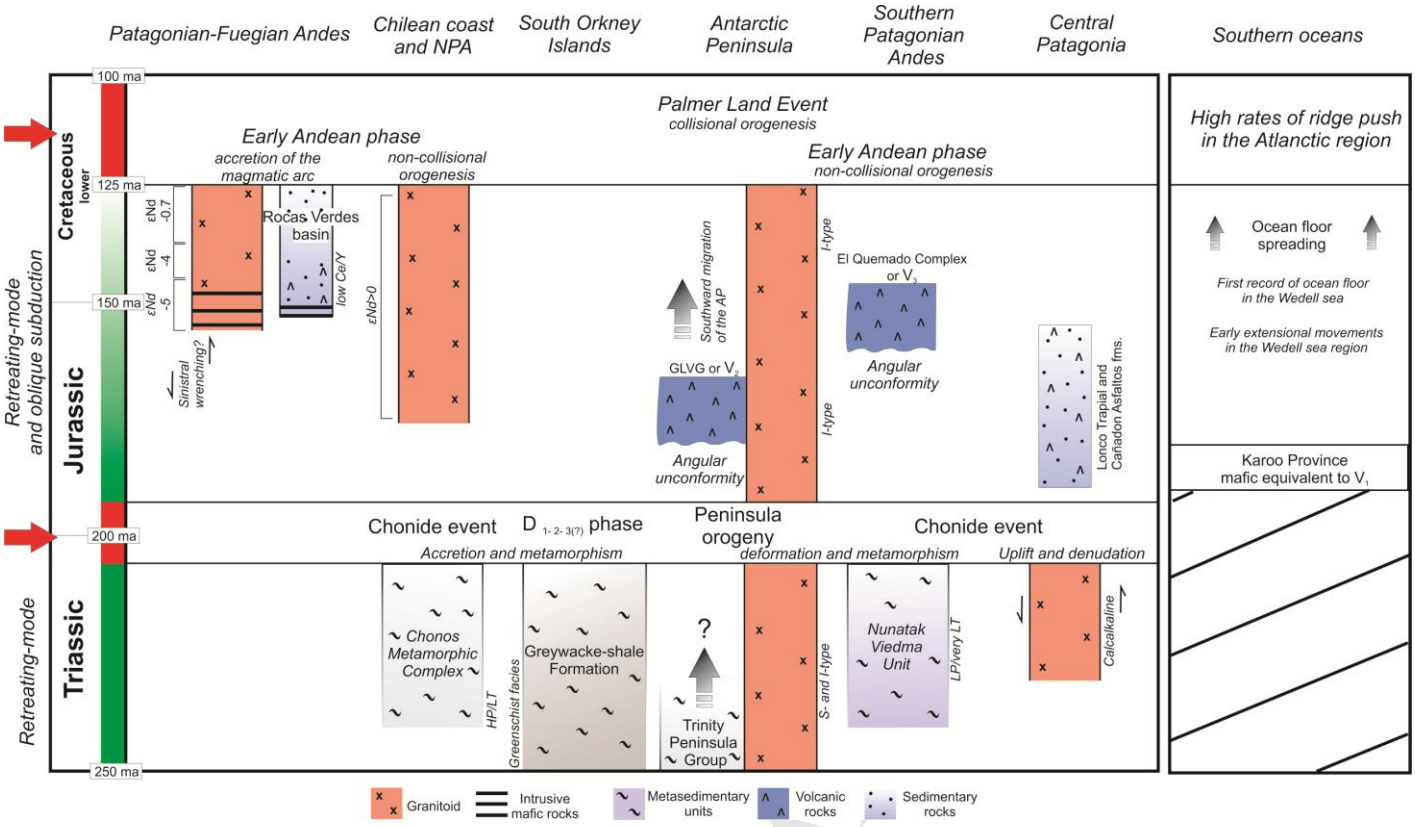

FIGURE 11

RESEARCH HIGHLIGHTS

- We recognized very-low grade metamorphic rocks on the Southern Patagonian Icefield.
- Late Triassic maximum depositional ages were constrained by zircon detrital ages.
- We propose to define the Nunatak Viedma Unit.
- A backarc setting is interpreted.
- Detrital zircon ages support Antarctic Peninsula-Patagonia Triassic connection.